CREB-TFDP3 Promotes Prostate Carcinoma Cell Growth by Inhibiting E2F1-Dependent Apoptosis

Rui Li
Xijing Hospital
Liu Yang
Xijing Hospital
Yinghong An
Air Force Medical Center
Lei Dong
Air Force Medical Center
Juan Wang
Xijing Hospital
Xiaoke Hao
Xijing Hospital
Yueyun Ma (mayueyun2020@163.com)
Air Force Medical Center https://orcid.org/0000-0001-5525-919X

Research

Keywords: PCa, CREB, TFDP3, E2F1, CRPC, CRISPR / cas9

Posted Date: November 12th, 2020

DOI: https://doi.org/10.21203/rs.3.rs-103662/v1

Abstract

Background

The cAMP-responsive element-binding protein (CREB) is a transcription factor that controls cell differentiation and survival. CREB is overexpressed and constitutively phosphorylated in several human cancers, including prostate cancer (PCa). However, the regulation of CREB in PCa remains to be deciphered. We previously demonstrated that TFDP3 negatively regulates E2F1 transactivation, which is important in PCa carcinogenesis. And 5 CREB binding sites were found in the upstream of TFDP3 promoter.

Methods

Luciferase and chromatin immunoprecipitation assays were used to determine the association between CREB and TFDP3. Immunohistochemical staining and immuno-cytofluorescence assays were performed to determine the expression of CREB and TFDP3 in a prostate cancer tissue microarray and cell lines. Cell lines stably expressing the wild-type, overexpression or knockout of CREB and TFDP3 were established. The protein expression of CREB and TFDP3 were detected by western blot analysis. CCK-8, TUNEL staining and cell cycle analysis were used to analyze the proliferation and apoptosis of the stable cell lines in vitro. The tumor growths were evaluated using nude mice xenograft models.

Results

Our results demonstrated that CREB could bind to the TFDP3 promoter and induce the transcription of TFDP3. Both CREB and TFDP3 were highly expressed in the androgen-independent cell line PC3 and prostate cancer tissues. Furthermore, *in vitro* and *in vivo* assays demonstrated that overexpression of CREB could promote cell proliferation and inhibit apoptosis in PC3 cell lines as determined using cell CCK-8 assays, flow cytometry, and western blotting assays. Knockout of CREB in PC3 cells resulted in a reduction in tumorigenicity in nude mouse xenograft models. Notably, the overexpression of CREB/TFDP3 in the LNCap cell line increased the progression of G1 cells to S phase, while knockout of CREB/TFDP3 arrested LNCaP AI+F cells at the G1 phase.

Conclusions

Taken together, our results suggested that CREB/TFDP3/E2F1 was involved in the pathogenesis of PCa. This provides novel insights into the mechanism of androgen-resistance in PCa.

Background

Prostate cancer (PCa) represents the most common malignancy in males in several countries and is the second leading cause of male death in China during the past decade (1). Androgen deprivation has been shown to be very successful for the treatment of hormone-sensitive PCa. However, the effect of androgen deprivation is reduced when tumor cells gradually reinitiate proliferation in an androgen-independent way.

The progression to castration-resistant prostate cancers (CRPC) is a major therapeutic challenge for prostate cancer patients and eventually leads to poor prognosis. However, the underlying mechanism of CRPC remains to be deciphered.

The E2F1 protein (E2F1) is a transcription factor that is involved in the cell cycle, replication, and apoptosis (2). E2F1 was identified as an essential target gene that could regulate the transcription of target genes in CRPC (2). In addition, the deregulation of E2F activity and early cell cycle progression has been implicated in aggressive prostate cancer (3, 4). The human transcription factor dimerization partner family member 3 (TFDP3) is a negative regulator of E2F that inhibits E2F-mediated transcriptional activation (5, 6). TFDP3 can inhibit E2F1-induced apoptosis while E2F1 antagonizes TFDP3-induced autophagy in the prostate cancer cell line, LNCaP (7). In our previous study, we demonstrated that TFDP3 was highly expressed in approximately 62.3% of all stages of prostate cancer. In addition, it was broadly expressed and corresponded with E2F1 levels(2). By inhibiting E2F1 activity, TFDP3 suppressed E2F1-mediated apoptosis and promoted the proliferation and tumorigenesis of PCa (2).

There are several cAMP-responsive element(CRE)-binding protein (CREB) binding sites on the upstream of the TFDP3 promoter. CREB has been identified to play an important role in cancer and has been associated with the overall survival and therapeutic response in cancer patients(8). The elevated expression of CREB is accompanied by enhanced cell proliferation, reduced sensitivity to apoptosis, increased angiogenesis, and radiation-induced differentiation (9), and are a result of CREB overexpression-mediated upregulation of downstream target genes of CREB that have CRE elements in their promoters. In human PCa, aberrant expression of CREB has been associated with PCa metastasis and/or androgen-independent progression(10). The majority of neuroendocrine differentiation (NED)-inducing stimuli, such as androgen depletion and irradiation act by increasing the intracellular levels of cAMP to activate protein kinase A (PKA) (12). Activated PKA is sufficient to induce neuroendocrine-like differentiation in LNCaP cells (13). CREB shRNA and/or a dominant-negative inhibitor of CREB (A-CREB) in LNCap cells have been shown to inhibit irradiation-induced NED (11). CREB has also been investigated as a drug target. Doxorubicin has been shown to increase CREB activation and induce prostate cancer drug resistance (12). CREB is a major regulator of cell proliferation in a wide variety of cells and acts via PKA (13). Furthermore, CREB has been demonstrated to be activated in Abiraterone acetate (AA) resistant cell lines (14), and CREB overexpression has been associated with dysregulated CDK-E2F activity in leukemias(15). E2F1 has been shown to directly regulate CREB expression(15), while treatment with the cyclin-dependent kinase (CDK) inhibitor AT7519, decreased the expression of CREB, and E2F target genes(15). Whether CREB plays a regulatory role in the TFDP3/E2F1 axis needs to be determined.

We hypothesized that CREB augments the TFDP3/E2F1 signaling pathway to have an anti-apoptotic role in CRPC. In this study, we demonstrated the binding profile of CREB to TFDP3 and showed that the CREB/TFDP3/E2F1 axis signaling pathway is involved in cell proliferation, apoptosis inhibition, tumorigenesis, and cell cycle entry.

Materials And Methods

Ethics statement

Based on the guidelines of the National Science Council of China, all study animals were maintained in an aseptic condition with a laminar airflow cabinet. All experimental procedures conformed to the guidelines of the Beijing Medical Experimental Animal Care Commission. The present study was approved by the Laboratory Animal Ethics Committee of the Air Force Medical University.

Cell culture

PC3 (androgen-independent, ATCC Cat# CRL-1435, RRID: CVCL_0035), LNCaP (androgen-sensitive, ATCC Cat# CRL-1740, RRID: CVCL_1379), LNCaP AI+F (androgen-independent, gift from Zhihua Tao's Lab)(16), and normal prostate stroma myofibroblast cell line WYMP-1 (ATCC Cat# CRL-2854, RRID:CVCL_3814) were used in this study. Cells were grown in RPMI-1640 medium (Gibco), supplemented with 10% fetal bovine serum (Gibco), or Charcoal-stripped fetal bovine serum (CS-FBS) (GeneTex, Inc. San Antonio, Texas), 100 IU penicillin and 0.1 mg/ml streptomycin (Sigma) at 37 °C in a humidified environment with 5% CO2.

Tissue microarray

The tissue microarrays were obtained from CRBRDI (Shaanxi Chaoying Biotec Co. LTD). The PCa microarray included 11 normal prostate samples (13.8%), 8 clinical-stage I samples (10%), 25 stage II samples (31.3%), 15 stage III samples (18.8%), and 21 hyperplasia samples (26.3%).

Plasmid Generation

A 2.0 kb sequence from the human TFDP3 promoter was generated by PCR using genomic DNA as a template that was extracted from the PC3 cell line. Primer sequences containing the NheI and HindIII restriction enzyme sites were used in the PCR (primer sequences are listed in Supplementary Table 1). Following enzymatic digestion with the restriction enzymes (NEB, New England Biolabs), the amplicon was sub-cloned into the pGL3-basic vector (Promega). In addition, we generated the promoter-CREB-mut construct, which contained the mutant type of the TFDP3 promoter. Sequencing was performed to verify all constructs before transfection. The pcDNA3.1-CREB (Invitrogen) was then generated in our lab. The primers for CREB used for PCR are listed in Table 1. A total of 6 different sets of siRNA sequences (home-317, home-434, home-719, home-577, home-725, home-1038) for CREB and TFDP3 were purchased from Shanghai GenePharma LTD. The sequences for CREB siRNAs are listed in table 1. pcDNA3.1-TFDP3 was generated in our laboratory as previously described (2).

Luciferase assays

A total of 1×10^6 cells (PC3, LNCaP, or WYMP-1) were seeded in 6 well plates and grown overnight before treatment. Co-transfection of expression plasmids with the TFDP3 core promoter was performed using Lipofectamine 3000 (Invitrogen) reagent according to the manufacturer's protocol. For promoter activity assessment, each well was transfected with 900 ng of the reporter constructs and 100 ng of a pRL-CMV

plasmid vector encoding Renilla luciferase (Promega). Renilla luciferase served as the internal control for transfection efficiency. Following 48 h of incubation, the cells were harvested and luciferase activity was measured using the Dual-Luciferase Reporter Assay System (Promega) according to the manufacturer's protocol. Each experiment was repeated at least 3 times, and each sample was tested in triplicate.

Chromatin immunoprecipitation assay

ChIP assays were performed using the ChIP kit (Millipore) according to the manufacturer's protocol. A total of 4 to 6×10^6 PC3 cells were washed and protein–DNA complexes were cross-linked in 1% formaldehyde in PBS for 10 min at 37 °C. Subsequently, the cells were collected and lysed in SDS lysis buffer (1% SDS, 10mM EDTA, 50 mM Tris-HCl, pH 8.1, and freshly added protease/phosphatase inhibitors). The chromatin was sonicated to shear the DNA to an average length of 300 to 700 bp using the Branson Low Power Ultrasonic Systems 2000 LPt/LPe sonicator. The DNA fragments were subsequently immunoprecipitated with 2μg antibody against CREB (Cell Signal Technology) or IgG. The precipitated DNA was extracted and amplified by PCR. The primer pairs were designed to bind to the CREB element in the TFDP3 promoter region. Primer sequences used in PCR are shown in Table 1. The soluble chromatin before immunoprecipitation was used as the input control. The PCR products were electrophoresed on a 3% agarose gel.

Western blotting analysis

Briefly, WPMY-1, PC3, and LNCap cells were lysed in RIPA lysis buffer (Beyotime) and total protein concentration was determined using the Pierce™ BCA Protein Assay Kit (Thermo). A total of 30 μg of protein was separated using a 10% SDS–PAGE, and then transferred onto PVDF membranes (Invitrogen). After incubation in blocking buffer (Invitrogen) for 2 h at room temperature, the membranes were incubated with antibodies for CREB (1:800, Abcam Cat# ab32515, RRID:AB_2292301), TFDP3(1:500, Abcam Cat# ab57342, RRID:AB_2202697) or β-actin(1:1000, A2228, Sigma) followed by incubation with a horseradish peroxidase (HRP)-conjugated secondary antibody (Cell Signal Technology). The catalog numbers of the primary antibodies are shown in Supplementary Table 2. Specific protein bands were detected using the Bio-Rad Image Lab system. Each band density was measured using the Image J software (java, National Institutes of Health: NIH) and normalized using the internal controls.

Immunohistochemistry (IHC) staining of tissue microarrays

Tissue slides were washed 2 times for 5 min in PBS and then blocked for endogenous peroxidases using 3% H_2O_2-methanol for 10 min at room temperature. Subsequently, primary antibodies against TFDP3 (1:50, Abcam Cat# ab57342, RRID: AB_2202697) and/or CREB (1:200, Abcam Cat# ab32515, RRID: AB_2292301) were incubated at 4 °C overnight. After washing, the membranes were incubated with anti-mouse/rabbit-HRP secondary antibody at room temperature for 30 min. Finally, DAB was used to visualize protein expression levels. Immunoreactivity scores (IRS) were calculated using the 0–3+ scale, where 0 indicated no staining; 0–1+ indicated trace staining that was weaker than 1+ and more intense than 0; 1+; 2+, and 3+ indicated increased intensities of staining. IRS was scored independently by two

pathologists who were blinded to the clinical data. The subregions, excluding necrosis, macrophages, and infiltrating neutrophils and lymphocytes were selected and scored. The intensity score for an array spot was the average of all sub-regions.

Immuno-cytofluorescence (ICF) staining of PCa cells

For ICF experiments, cell-coated slides were washed with 0.01 M PBS and fixed with 4% cold paraformaldehyde in phosphate buffer (pH 7.4). The slides were blocked with 0.01 M PBS containing 3% BSA and 0.3% Triton X-100 for 30 min and then incubated with rabbit anti-CREB (1:800, Abcam Cat# ab32515, RRID: AB_2292301) and mouse anti-TFDP3 (1:500, Abcam Cat# ab57342, RRID: AB_2202697) at 4°C overnight. Following three washes with 0.01 M PBS, the slides were incubated with the corresponding secondary antibodies conjugated with FITC (1:100, BBI Life Sciences) and/or Cy3 (1:400, BBI Life Sciences) for 1 h at room temperature. Nuclei were counterstained using DAPI (1:500, Beyotime). Sections were examined and photographed using a confocal microscope (FV1000, Olympus).

Apoptosis assay

PC3 cells (6×10^5 cells/well) were stained with Annexin V-FITC using the Annexin V FITC Apoptosis Detection Kit (Millipore). The cells were then washed twice in PBS and resuspended in binding buffer. 50 µl of the cell suspension was then stained with 10 µl of Annexin V-FITC and gently vortexed and incubated in the dark for 15 min at room temperature. Finally, 5 µl of Propidium Iodide (PI) was added, and the suspension was incubated in the dark for an additional 5 min at room temperature. Following the addition of 400 ul of binding buffer to each tube, cells were analyzed by flow cytometry (CantoII, BD).

TUNEL staining was performed according to the Dead END™TUNEL system instruction manual (Promega, Catalog number selected: G3250) to determine the percentage of cellular apoptosis. Briefly, PC3 cells were fixed to a microscope slide by immersing in 4% methanol-free formaldehyde in PBS for 25 minutes at 4°C. Then, cell sections were permeabilized with 0.2% Triton® X-100 (Sigma) for 5 min and rinsed 2 times with PBS. The cells were then covered with 100µl of Equilibration Buffer and incubated at room temperature for 5–10 min. The Equilibration Buffer was then removed and 50µl of rTdT incubation buffer was added to the cells covering a $5cm^2$ area. The slides were then covered with aluminum foil and incubated at 37°C for 60 min inside a humidified chamber. The reaction was terminated by immersing the slides in 2X SSC for 15 min at room temperature. The slides were then stained by immersing in 40ml of propidium iodide solution diluted to 1µg/ml in PBS for 15 minutes at room temperature in the dark. Samples were immediately analyzed under a fluorescence microscope for green fluorescence of fluorescein at 520 ± 20nm, red fluorescence of propidium iodide at >620nm, and blue DAPI at 460nm. Nuclei were counterstained with Hoechst33342 (1:5000, Sigma).

Cell Proliferation Assay

Cell proliferation was measured using the Cell Counting Kit-8 (CCK-8) (Dojindo Laboratories, Kumamoto, Japan) according to the manufacturer's protocol. Briefly, the cells were seeded in 96-well plates (2×10^3

cells /well) in triplicate and incubated for 12 h. The cells were then transfected with pcDNA3.1-CREB and/or siRNA-CREB for 24, 48, and 72 h, followed by the addition of 10 μl of CCK-8 solution to each well. Following incubation at 37 °C for 1.5 h, the absorbance of each sample at 450 nm was measured using a microplate reader (Tecan, Austria).

Cell cycle analysis

The effect of CREB and TFDP3 on LNCaP and LNCaPAI+F on cell cycle progression were determined on a fluorescence-activated cell sorter (FACS) using the Cell Cycle Assay kit (Fluorometric-Green, ab112116) according to the manufacturer's instructions. A total of 1×10^6 cells were collected in flow tubes, washed with PBS, and then stained with Nuclear Green CCS1. After cells were incubated in the dark for 15 minutes, ten thousand cells were analyzed by flow cytometry (CantoII, BD). Cells stained with Nuclear Green CCS1 were monitored using a flow cytometer set at an Ex/Em of 490 nm/520 nm. All experiments were performed in triplicate.

Construction of CREB1/TFDP3 knockout cell lines using CRISPR / cas9

sgRNAs targeting CREB1 and TFDP3 were designed using CRISPR DESIGN (http://crispr.mit.edu/). The transfer plasmid lentiCRISPR-CREB and lentiCRISPR-TFDP3 were obtained from TsingKe Biotechnology Co., Ltd. Briefly, three targets for CREB1 and TFDP3 were designed. The target sequences were as follows: Target1: GGGCAGACAGTTCAAGTCCA, Target2: GGGCTTGAACTGTCATTTGT and Target3: GGAGCCGAGAACCAGCAGAG for CREB1; Target1: GCCGGGCAGCACAACAGGAA, Target2: GCCGTCTTTCCATGAAGGTC and Target3: GGAGGTGTGTTCACGACGGC for TFDP3. The corresponding lentiCRISPR vectors were constructed to synthesize oligos for lentiCRISPR-CREB-T1, lentiCRISPR-CREB-T2, lentiCRISPR-CREB-T3 and lentiCRISPR-TFDP3-T1, lentiCRISPR-TFDP3-T2, lentiCRISPR-TFDP3-T3, respectively. CRISPR / cas9 activity was measured using Luciferase SSA. The strongest fluorescence vectors were selected for Lentivirus packaging. The specific target sequences were amplified and cloned into a Lentivirus plasmid packaging system. DNA sequence analysis was used to verify the sequences.

Animal experiments

Six-week-old female BALB / C nude mice (from Vital River, Beijing, China) were randomly divided into three groups according to weight (n=10 per group). PC3, PC3 with lentiCRISPR-CREB1, or PC3 with lentiCRISPR-TFDP3 cell lines (1×10^7) were suspended in 0.1 ml of PBS and injected subcutaneously into the right abdominal flank of mice using 26G needles. The tumor volume was observed daily. The tumor volume was calculated using the following formula: volume(mm^3)=(width)^2(mm^2)×length(mm)/2. Relative tumor volume (RTV): RTV= V_t / V_0, where V_0 is the starting tumor volume and V_t is the tumor volume at each measurement. On day 19, tumors were harvested from the right abdominal flank of the mouse, weighed, photographed, fixed in formalin, and embedded in paraffin for sectioning.

Statistical analyses

Statistical analyses were performed using GraphPad Prism 5 software (GraphPad Software Inc., La Jolla, CA, USA) and IBM SPSS software 21.0. Statistical differences between groups were determined using one-way ANOVA and unpaired t-tests. Correlation was analyzed using the Spearman's rank test. Results were presented as mean (central values) ± SD (error bars). P values of less than 0.05 were considered significant. Three levels of significance (*P<0.05; **P<0.01; ***P<0.001) were applied for all tests.

Results

CREB binds to the TFDP3 promoter

The TFDP3 promoter sequence from -2404 was analyzed using the PROMO 3.0 software (http://alggen.lsi.upc.es/). We observed multiple response elements, including 5 CREB binding sites in the region between -141 and -47(Fig.1A). We focused on determining CREB function as it relates to TFDP3 expression. Luciferase reporter assays demonstrated that overexpression of CREB dramatically enhanced the luciferase activity of the reporter plasmid. In contrast to the TFDP3 promoter plasmid, the mutant version of the plasmid i.e., pGL3-TFDP3-promoter–mut, did not show an increase in luciferase activity following CREB overexpression (Fig.1B).

In addition, ChIP assays demonstrated that the anti-CREB antibody could immunoprecipitate DNA fragments of the TFDP3 promoter, as demonstrated by the presence of a positive signal that was similar in size to the amplicon generated with input DNA (Fig. 1C). Collectively, these results demonstrated that the upregulation of CREB significantly enhances TFDP3 activity.

TFDP3 and CREB is expressed in human prostate cells and tissues

Western blotting and immunofluorescence assays were used to measure expression levels of CREB and TFDP3 in prostate cancer cells. CREB and TFDP3 expression was localized in the nucleus and their average protein levels were significantly higher in PC3 compared to MPMY-1 and LNCaP cells (Fig. 2C). In addition, TFDP3 was highly expressed in PC3 not only in the nucleus but also in the cytoplasm (Fig. 2A). Due to the androgen-independent characteristics of PC3, it implied that TFDP3 and CREB may play a role in androgen-independent cancer progression.

To evaluate whether CREB correlates clinically with prostate cancer progression, immunohistochemistry on tissue microarrays was performed to measure the expression levels of CREB and TFDP3 in normal prostate tissue, prostate hyperplasia, and different grades of human prostate cancers (Fig. 2D). Our results demonstrated that CREB expression was associated with PCa grade at equivalent expression levels in PCa tissue samples (P < 0.01, rs =0.354) (Fig. 2D, E). Expression levels of TFDP3 in human prostate cancer were considerably higher compared to normal and benign prostatic hyperplasia tissues, notably in tumors with a higher stage (P<0.05, rs=0.233) (Fig. 2D and F). In addition, immunohistochemistry demonstrated strong positive staining for TFDP3 in 45 out of 48 (89.58%) samples of clinical PCa tissues (Supplementary Table 3). The expression levels of CREB measured in the same tumor samples correlated with the expression levels of TFDP3 (P < 0. 01, rs = 0.869).

CREB regulates TFDP3 expression

The silencing efficiency of the different CREB-siRNAs was evaluated by western blotting analysis and showed that CREB-home-317 was the most effective in downregulating CREB expression (Fig. 3A). CREB knockdown significantly downregulated the expression of TFDP3 in PC3 cells (Fig. 3A and B). In contrast, pcDNA3.1-CREB transfected PC3 showed a significant increase in expression of TFDP3 protein levels (Fig. 3C and D).

CREB localization was then determined using ICF. CREB was found to be localized in the nucleus following transfection with pcDNA3.1-CREB. Transfection with pcDNA3.1-CREB increased in expression levels of TFDP3, however, CREB knockdown with CREB siRNA-317 resulted in a decrease in fluorescence intensity for both CREB and TFDP3 (Fig.3E).

CREB affects the proliferation and apoptosis of prostate cancer cells

To investigate the role of CREB-TFDP3 interaction, proliferation, and apoptosis in prostate cancer cells were evaluated after exogenous overexpression and/or endogenous knockout of CREB.

Our previous work demonstrated that TFDP3 could inhibit PC3 apoptosis induced by E2F1(17). In the present study, CREB could decrease the number of TUNEL-positive PC3 cells ($P<0.05$), and CREB knockout increased the percentage of TUNEL positive PC3 cells ($P<0.05$) (Fig. 4A and 4B). In addition, flow-cytometry analysis demonstrated that late apoptosis rates were lower compared to cells in the control group. CREB transfection decreased late apoptosis from 16.5% to 13.2% (Fig. 4C), while the total rate of apoptosis decreased significantly, $P<0.01$(Fig. 4D). Similarly, the downregulation of CREB by siRNACREB increased apoptosis, $P<0.001$ (Fig. 4D). The early phase apoptosis rates increased from 3.0% to 4.9%, while late phase apoptotic rates decreased from 24.5% to 16.5% (Fig. 4C). Related apoptotic proteins in the E2F1 pathway were then evaluated after overexpression or silencing of CREB. These proteins included bad, p-bad, puma, bax, bid, and bik proteins (Fig. 4E). Bad, puma, bax, bid, and bik are pro-apoptotic proteins, while p-bad is anti-apoptotic due to its phosphorylation state. As shown in Fig. 4F, the silencing of CREB resulted in an obvious increase in expression levels of pro-apoptotic proteins and a decrease in expression levels of anti-apoptotic proteins. These results strongly suggested that CREB affects apoptosis in the PC3 cell line. CCK-8 assays also demonstrated that overexpression of CREB increased the proliferation rates of PC3 prostate cancer cells while silencing CREB expression reduced proliferation rates (Fig. 4G). Taken together, our data suggest that CREB plays an important role in promoting proliferation and inhibiting apoptosis in PCa cells.

CREB-dep and TFDP3-dep inhibits tumor growth in PC3 xenograft mouse models

We next functionally validated the role of CREB and TFDP3 in PC3 tumorigenicity *in vivo*. PC3 cells were used to establish stable cell lines expressing shRNAs targeting CREB and TFDP3 using CRISPR/cas9. Vectors that had the highest fluorescence intensities as measured by Luciferase SSA were selected as target sequences, i.e., CREB-T1 and TFDP3-T3 (Fig. 5A and B). PC3, PC3 with lentiCRISPR-CREB, and PC3

with lentiCRISPR-TFDP3 cell lines were then injected subcutaneously into the right abdominal flank of mice to establish the PC3 xenograft mouse model. No obvious adverse effects were observed in terms of body weights during the studies (Fig. 5E). For mice injected with PC3+lentiCRISPR-CREB and PC3+lentiCRISPR-TFDP3, tumor growth was reduced compared to mice injected with PC3 cells (Fig. 5C and D). At the end of the study, tumors were harvested and weighted. As shown in Fig.5F, the tumor weight of mice injected with PC3+lentiCRISPR-CREB and PC3+lentiCRISPR-TFDP3 were significantly lower compared to tumors from mice in the vehicle control group, $P<0.001$. This demonstrates that CREB-dep and TFDP3-dep could reduce tumorigenicity in our xenograft tumor model.

CREB/TFDP3 overexpression and knockout affects the cell cycle in androgen-dependent or independent prostate cancer cells

E2F transcription factor is important for cell cycle entry and proliferation (18). The binding of CREB and TFDP3 to E2F1 may modulate cell cycle entry. CREB and TFDP3 affect proliferation, apoptosis, and tumorigenicity by regulating the transcription of E2F1 in prostate cancer cells. We investigated whether CREB and TFDP3 play a role in cell cycle progression. As shown in Fig. 6A, CREB and TFDP3 overexpression in the LNCap cell line increased G1 to S phase progression. Androgen withdrawal may drive prostate cancer cells into CRPC, which is a major therapeutic challenge for prostate cancer patients. The LNCap AI+F cell lines were used to determine the effects of CREB and TFDP3 on the cell cycle. As shown in Fig. 6B, knockout of CREB and TFDP3 induced a substantial accumulation of cells in the G1 stage of the cell cycle in LNCaP AI+F cells, while androgen withdrawal and CREB/TFDP3 knockout arrested LNCaP AI+F cells at the G1 phase.

Discussion

CREB belongs to the family of basic leucine zipper (bZIP) proteins and has been identified as a crucial transcription factor (19). In most solid tumors, the expression of CREB correlates with poor patient prognosis. It is located downstream of several growth signaling pathways and is involved in cell survival, proliferation, differentiation, and tumorigenesis. Over 4,000 CREB targets have been identified to be involved in tumor phenotype, clonal formation, increased proliferation, and protooncogene transformation (12,22). Multiple signaling pathways have been identified to be involved in CREB activation via CREB-binding sites. The transcriptional activity of CREB is induced by various kinases such as PKA, PKB/AKT, and MAPK due to its reversible phosphorylation sites at various serine residues. Roflumilast can enhance cisplatin sensitivity and reverse cisplatin resistance in ovarian cancer cells via the activation of the cAMP/PKA/CREB pathway (20).

In this study, we identified multiple response elements including a CREB binding site at the region between -141 and -47 of the TFDP3 promoter. CREB can bind to the TFDP3 promoter and stimulate TFDP3 transcription. Our recent study demonstrated that CREB transcriptional activity was associated with TFDP3. Overexpression of CREB significantly enhanced the luciferase activity of the reporter plasmid pGl3-TFDP3 promoter in PC3 cells. TFDP3 was positively regulated by CREB at the transcriptional and

translational level as determined by CREB siRNA and CREB over-expressing assays. Regulation of TFDP3 by CREB suggests crosstalk between the CREB and TFDP3 signaling cascade. We are the first to demonstrate TFDP3 and CREB expression simultaneously in the same prostate cancer tissue. However, not all tumor tissues express high levels of CREB and TFDP3. This may be related to the activation of downstream target genes and the tumor microenvironment. Compared to MPMY-1 and LNCaP cell lines, the protein levels of CREB and TFDP3 were significantly higher in the PC3 cell line. A previous study suggested that E2F1 and CREB cooperatively regulate the transcriptional activity of certain cell cycle genes (15). E2F1 can regulate a large number of genes involved in diverse cellular processes, such as replication, apoptosis, checkpoint control, and DNA repair (21). We previously demonstrated that E2F1 could regulate the expression of TFDP3, while TFDP3 could negatively regulate E2F1 by inhibiting DNA binding and E2F1 transactivation (2). Hence, the binding of CREB/TFDP3 and upregulation of CREB may inhibit E2F1-dependent apoptosis by enhancing the activity of TFDP3.

CREB has been demonstrated to be involved in several tumor types such as leukemia, ovarian cancer, gliomas, and prostate cancer (25,26). Higher CREB expression levels are often associated with oncogenic transformation. This is via the modulation of genes involved in cell proliferation, cell cycle, apoptosis, and tumor development. Overexpression of CREB in transgenic mice has been demonstrated to induce myeloproliferative disorders(22). Numerous studies have suggested CREB to be associated with apoptosis. CREB has been demonstrated to inhibit apoptosis of acute promyelocytic leukemia cells induced by arsenic via caspase-3 (23). In UV-induced apoptosis, CREB induces C-FLIPL and MKP-1 and exerts a protective effect (24). In colon cancer, CREB was found to inhibit apoptosis through the ERK1/2, p38, and MAPK pathways(25). CREB has also been demonstrated to exert anti-apoptotic properties in different tissues under different conditions. Downregulation of CREB suppresses cell growth and survival and induces apoptosis in NSCLC□esophageal squamous cell carcinoma (ESCC) and human pre-B acute lymphoblastic leukemia (25,31,32). Our results demonstrated that both CREB and TFDP3 were highly expressed in the androgen-independent PC3 cell line and clinical prostate cancer tissues. This was especially true in high grade cancers. Overexpression or silencing of CREB/TFDP3 could regulate proliferation and apoptosis of the PC3 cell line. The role of CREB in promoting cell proliferation and inhibiting apoptosis was consistent with that of TFDP3. This could partly explain the mechanism of CREB involvement in apoptosis. Similarly, knockout of CREB in PC3 cells resulted in reduced xenograft tumorigenicity in nude mice. We and others have previously demonstrated that TFDP3 is highly expressed in prostate cancer tissues, and not expressed or lowly expressed in normal tissues (2). TFDP3 inhibits the DNA binding, E2F1 transactivation and E2F1-dependent apoptosis (2,6). These findings indicate that TFDP3 may be connected with CREB and E2F1. CREB augments the TFDP3/E2F1 signaling pathway required for the progression of PCa. Adequate CREB expression could induce TFDP3 expression to block E2F1-mediated apoptosis. CREB specific shRNA and CREB inhibitors, such as lapatinib and KG501, has been shown to reverse the transformed phenotype and growth characteristics of breast cancer cells (26). Our results support the rationale of targeting CREB or CREB related pathways for the treatment of cancer (27, 28).

With regards to the treatment of hormone-sensitive PCa, androgen deprivation therapy (ADT) is the preferred treatment option. However, continuous ADT will eventually lead to androgen resistance which eventually results in CRPC and lead to treatment failure (12). During ADT progression, CREB is activated and significantly increases in expression (12,14). Aberrant expression of CREB has been associated with androgen-independent progression, which ultimately increases androgen receptor (AR) transcriptional levels (10, 29). During this stage, AR is continuously expressed and is likely to mutate. AR overexpression is one of the major reasons for CRPC(30). AR gene amplification has been observed in approximately 80% of CRPC cases (31). Higher CREB expression levels increase the tumorigenicity of LNCaP cells in castrated mouse tumor models (12,14,36). Androgen withdrawal and the CREB/TFDP3 axis in PCa may drive prostate cancer cells into CRPC. We hypothesized whether the CREB/TFDP3/E2F1 signaling pathway may be involved in the survival of androgen-sensitive or resistant cells. Using LNCap and LNCap AI+F cell lines to mimic androgen-dependent and androgen-independent (castration) tumors, changes in the cell cycle was investigated. Our results demonstrated that overexpression of CREB/TFDP3 in the LNCap cell line accelerated G1 to S phase progression, while knockout of CREB/TFDP3 arrested LNCaP AI+F cells at the G1 phase. These findings demonstrated that androgen and the increase in CREB/TFDP3 expression could promote cell cycle entry and subsequently cell proliferation. Absence of androgen and the decrease in CREB/TFDP3 expression arrested cell cycle entry. This suggested a partial reversal of castration resistance. Hence, CREB/TFDP3 amplifications or overexpression represents a resistance mechanism in PCa. The expression and regulation on PCa cell growth by CREB/TFDP3 indicated the involvement in castration resistant prostate cancer.

E2F1 is a transcription factor required for cell cycle progression and apoptosis (2). Dysregulation of E2F1 leads to unrestrained cell cycle progression in prostate cancer cells(32). Overexpression of E2F1 has been shown to sensitize tumor cells to etoposide-induced apoptosis in LNCaP cells(33). TFDP3 has been shown to inhibit E2F1-induced apoptosis in LNCaP cells (2). Hence, the expression of CREB/TFDP3 and the deregulation of E2F1 induced by increased expression of CREB/TFDP3 under androgen-dependent or independent conditions corporately leads to uncontrolled cell cycle progression in PCa cells.

Conclusions

In summary, our findings uncovered a novel biological role and regulatory mechanism of the CREB/TFDP3/E2F1 signaling pathway as it relates to the developmental mechanism of androgen-resistance in PCa. In addition, we demonstrated the potential role of CREB and TFDP3 as novel prognostic biomarkers and therapeutic targets for PCa.

Abbreviations

PCa: prostate cancer; CREB: cAMP-responsive element-binding protein; TFDP3: the human transcription factor dimerization partner family member 3; CRPC: castration-resistant prostate cancers; NED: neuroendocrine differentiation; AA: cAMP Abiraterone acetate; CDK: cyclin-dependent kinase; IHC : Immunohistochemistry; IRS: Immunoreactivity scores; ICF: Immuno-cytofluorescence; PI: Propidium

Iodide; FACS: fluorescence-activated cell sorter; CRISPR / cas9: clustered regularly interspaced short palindromic repeats and CRISPR-associated protein-9 nuclease ; ChIP: chromatin immunoprecipitation; bZIP: basic leucine zipper; NSCLC: non-small cell lung cancer; ESCC: esophageal squamous cell carcinoma; ADT: androgen deprivation therapy; AR: androgen receptor; PKA: protein kinase A; A-CREB: a dominant-negative inhibitor of CREB

Declarations

Acknowledgements

We would like to acknowledge the helpful suggestions concerning this study received from our colleagues.

Funding

This work was supported by the National Science Nature Foundation of China (Grant No.81272619)

Ethics approval and consent to participate

The present study was approved by the Ethics Committee of the Air Force Medical University (No. XJYYLL-2013116). All experimental procedures conformed to the guidelines of the Beijing Medical Experimental Animal Care Commission. And based on the guidelines of the National Science Council of China, all study animals were maintained in an aseptic condition with a laminar airflow cabinet.

Consent for publication

Not applicable.

Availability of data and material

The datasets are available. All data were generated and analyzed in the current study by the corresponding author on reasonable request. All materials are properly obtained and certified.

Competing interests

The authors declared no conflicts of interest exist in the current study.

Authors' contributions

Rui Li and Liu Yang performed experiments and interpreted results of experiments. Yinghong An participated in the the animal studies, molecular biology experiments and drafted the manuscript. Lei Dong participated the cell-lines construction. Juan Wang participated in cell culture and performed the statistical analysis. Xiaoke Hao participated in the design and coordination research. Yueyun Ma conceived of the study and draft the manuscript. All authors read and approved the final manuscript.

Authors' information

1 The Department of Clinical Laboratory Medicine, Xijing Hospital, Air Force Medical University, Xi'an, China. 2 The Department of Clinical Laboratory, Air Force Medical Center, Beijing, China.

References

1. Chen W, Zheng R, Baade PD, et al. Cancer statistics in China, 2015. CA A Cancer J Clin 2016; 66.
2. Zhou Q, Wang C, Zhu Y, et al. Key Genes And Pathways Controlled By E2F1 In Human Castration-Resistant Prostate Cancer Cells. Onco Targets Ther 2019; 12: 8961-76.
3. Zhang Y, Song X, Herrup K. Context-dependent functions of E2F1: cell cycle, cell death, and DNA damage repair in cortical neurons. Molecular Neurobiology 2020; 57: 2377-90.
4. Wang F MA, Tang J, Zhang QJ , Yan JF, Wang YP , Di CX , Lu G microRNA-16-5p enhances radiosensitivity through modulating Cyclin D1/E1-pRb-E2F1 pathway in prostate cancer cells. J Cell Physiol 2019; 234: 9.
5. Qiao H, Stefano LD, Tian C, et al. Human TFDP3, a Novel DP Protein, Inhibits DNA Binding and Transactivation by E2F. Journal of Biological Chemistry 2007; 282: 454-66.
6. Tian C, Lv D, Qiao H, et al. TFDP3 inhibits E2F1-induced, p53-mediated apoptosis. Biochemical & Biophysical Research Communications 2007; 361: 0-25.
7. Ren LF, Yue-Yun MA, Yue QH, Ming-Quan SU. Effects of TFDP3 on regulating the autophagy and apoptosis of LNCaP cells. Chinese Journal of Cellular & Molecular Immunology 2012; 28: 347.
8. Steven A, Friedrich M, Jank P, et al. What turns CREB on? And off? And why does it matter? Cell Mol Life Sci 2020; 10: 10.1007/s00018-020-3525-8.
9. Suarez CD, Deng X, Hu CD. Original Article Targeting CREB inhibits radiation-induced neuroendocrine differentiation and increases radiation-induced cell death in prostate cancer cells. American Journal of Cancer Research 2014; 4: 850-61.
10. Comuzzi B, Lambrinidis L, Rogatsch H, et al. The Transcriptional Co-Activator cAMP Response Element-Binding Protein-Binding Protein Is Expressed in Prostate Cancer and Enhances Androgen- and Anti-Androgen-Induced Androgen Receptor Function. Am J Pathol 2003; 162: 233-41.
11. Sang M, Hulsurkar, M., Zhang, X., Song, H., Zheng, D., Zhang, Y., Li, M., Xu, J., Zhang, S., Ittmann, M., & Li, W. . GRK3 is a direct target of CREB activation and regulates neuroendocrine differentiation of prostate cancer cells. Oncotarget 2016; 7: 45171-85.
12. Mallappa S, Neeli PK, Karnewar S, Kotamraju S. Doxorubicin induces prostate cancer drug resistance by upregulation of ABCG4 through GSH depletion and CREB activation: Relevance of statins in chemosensitization. Molecular Carcinogenesis 2019; 58: 1118-33.
13. Zou S, Wang X, Deng L, et al. CREB, another culprit for TIGAR promoter activity and expression. Biochem Biophys Res Commun 2013; 439: 481-6.

14. Pan W, Zhang Z, Kimball H, Qiu F, Kantoff PW. The effect of abiraterone acetate treatment on CREB and the development of abiraterone acetate resistance in prostate cancer cells. Journal of Clinical Oncology 2020; 38.
15. Chae H-D, Mitton B, Sakamoto K. CREB Regulates Cell Cycle Progression through RFC3-PCNA Axis in Acute Myeloid Leukemia. Blood 2014; 124: 881-.
16. Xu G, Wu J, Zhou L, et al. Characterization of the small RNA transcriptomes of androgen dependent and independent prostate cancer cell line by deep sequencing. PLoS One; 5: e15519.
17. Li R, Ma YY, Xin YJ, Diao YJ, Hao XK. Role for E2F1 in the regulation of transcription factor dimerization partner-3 expression and apoptosis in prostate cancer PC3 cells. Chinese Journal of Cancer Biotherapy 2014; 21: 125-9.
18. Wong JV, Dong P, Nevins JR, Matheyprevot B, You L. Network calisthenics: control of E2F dynamics in cell cycle entry. Cell Cycle 2011; 10: 3086-94.
19. André Steven1 BS. Control of CREB expression in tumors: from molecular mechanisms and signal transduction pathways to therapeutic target. Oncotarget 2016; 7: 35454-65.
20. Gong S, Chen Y, Meng F, et al. Roflumilast enhances cisplatin-sensitivity and reverses cisplatin-resistance of ovarian cancer cells via cAMP/PKA/CREB-FtMt signalling axis. Cell Prolif 2018; 51: e12474.
21. Gong S, Chen Y, Meng F, Zhang Y, Fei W. Roflumilast restores cAMP/PKA/CREB signaling axis for FtMtmediated tumor inhibition of ovarian cancer. Oncotarget 2017; 8: 112341-53.
22. Cheng JC, Kinjo K, Judelson DR, Chang J, Sakamoto KM. CREB is a critical regulator of normal hematopoiesis and leukemogenesis. Blood 2008; 111: 1182-92.
23. Safa M, Mousavizadeh K, Noori S, Pourfathollah A, Zand H. cAMP protects acute promyelocytic leukemia cells from arsenic trioxide-induced caspase-3 activation and apoptosis. Eur J Pharmacol 2014; 736: 115-23.
24. Zhang J, Wang Q, Zhu N, et al. Cyclic AMP inhibits JNK activation by CREB-mediated induction of c-FLIPL and MKP-1, thereby antagonizing UV-induced apoptosis. Cell Death Differ 2008; 15: 1654-62.
25. Nishihara H, Hwang M, Kizaka-Kondoh S, Eckmann L, Insel PA. Cyclic AMP Promotes cAMP-responsive Element-binding Protein-dependent Induction of Cellular Inhibitor of Apoptosis Protein-2 and Suppresses Apoptosis of Colon Cancer Cells through ERK1/2 and p38 MAPK. J Biol Chem 2004; 279: 26176-83.
26. André Steven SL, Chiara Massa, Manuela Iezzi, Rossano Lattanzio, Alessia Lamolinara, Jürgen Bukur, Anja Müller, Bernhard Hiebl, Hans-Jürgen Holzhausen, Barbara Seliger. HER-2/neu Mediates Oncogenic Transformation via Altered CREB Expression and Function. Mol Cancer Res 2013; 11: 1462-77.
27. Wang Y, Zhang J, Han M, et al. SMND-309 promotes neuron survival through the activation of the PI3K/Akt/CREB-signalling pathway. Pharm Biol 2016; 54: 1982-90.
28. Salmaninejad A, Zamani MR, Pourvahedi M, Golchehre Z, Rezaei N. Cancer/Testis Antigens: Expression, Regulation, Tumor Invasion, and Use in Immunotherapy of Cancers. Immunol Invest

2016; 45: 619-40.

29. Grossmann ME, Huang H, Tindall DJ. Androgen Receptor Signaling in Androgen-Refractory Prostate Cancer. J Natl Cancer Inst 2001; 93: 1687-97.
30. Henrique B da Silva EPA, Eduardo L Nolasco, Nathalia C de Victo, Rodrigo Atique, Carina C Jank, Valesca Anschau, Luiz F Zerbini, Ricardo G Correa. Dissecting Major Signaling Pathways throughout the Development of Prostate Cancer. Prostate Cancer 2013; 2013: 920612.
31. Kati K Waltering AU, Tapio Visakorpi. Androgen receptor (AR) aberrations in castration-resistant prostate cancer. Mol Cell Endocrinol 2012; 360: 38-43.
32. Jung Nyeo Chun MC, Soonbum Park, Insuk So, Ju-Hong Jeon. The conflicting role of E2F1 in prostate cancer: A matter of cell context or interpretational flexibility? Biochim Biophys Acta Rev Cancer 2020; 1873: 188336.
33. Libertini SJ, Tepper CG, Guadalupe M, Lu Y, Asmuth DM, Mudryj M. E2F1 expression in LNCaP prostate cancer cells deregulates androgen dependent growth, suppresses differentiation, and enhances apoptosis. Prostate 2006; 66: 70-81.

Figures

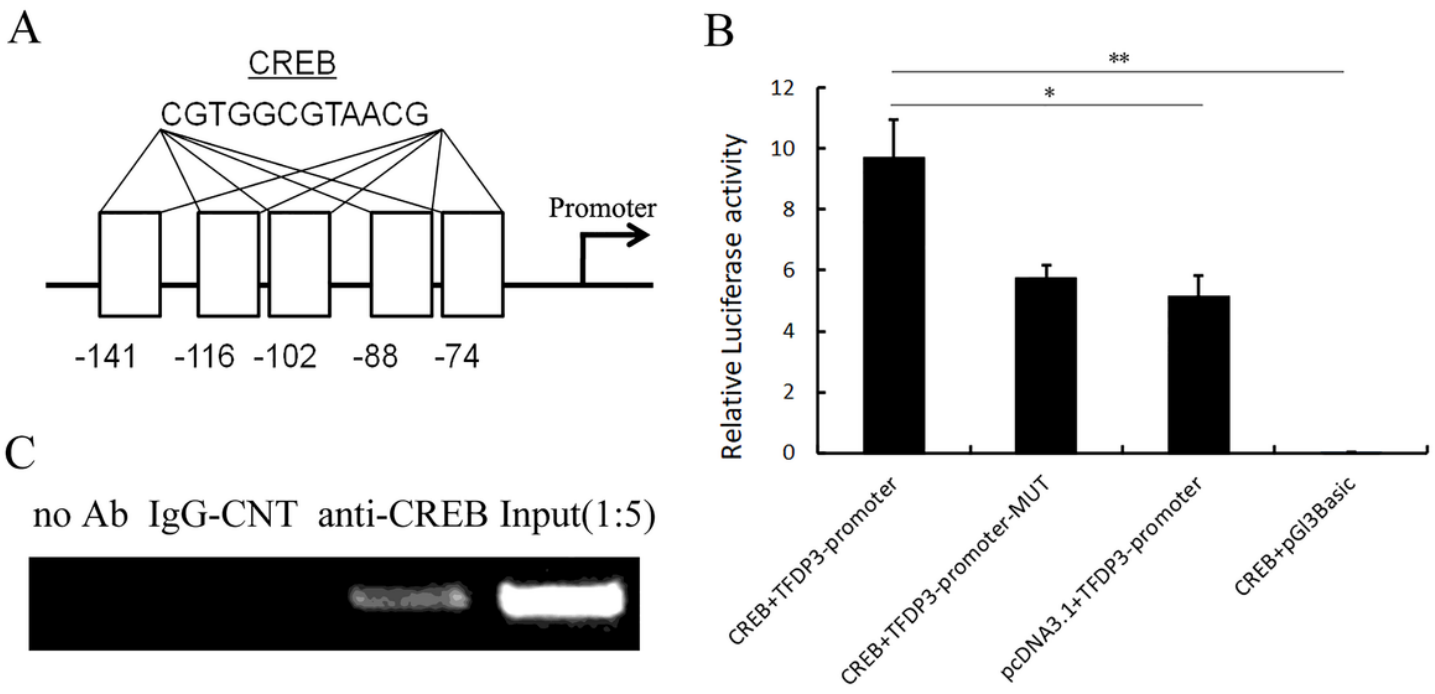

Figure 1

Luciferasereporterand ChIP assay analysis of the physical interaction between the putative CRE motif and the transcription factor, CREB. A. All constructs were transfected in the cells and the activity of the promoters was measured. The data are presented as the meanfirefly/Renilla luciferase ratio relative to the

activity of the wild construct (designated as 100%). Eachpoint corresponds to the mean ± SD of three assays that were conducted in triplicate. The asterisks indicate statistical significance (P < 0.05) between the groups. B. ChIP assay was used to examine the interactionbetween the TFDP3 promoter and CREB. The experiments were conducted with chromatin derived from cell lines. Immunoprecipitated chromatin was used for the PCR assay usingspecific primers and the amplicon was resolved on a 3% agarose gel. The input DNA was used as a positive control for amplification. C. Schematic chart of the binding sites up-stream of the TFDP3 promoter.

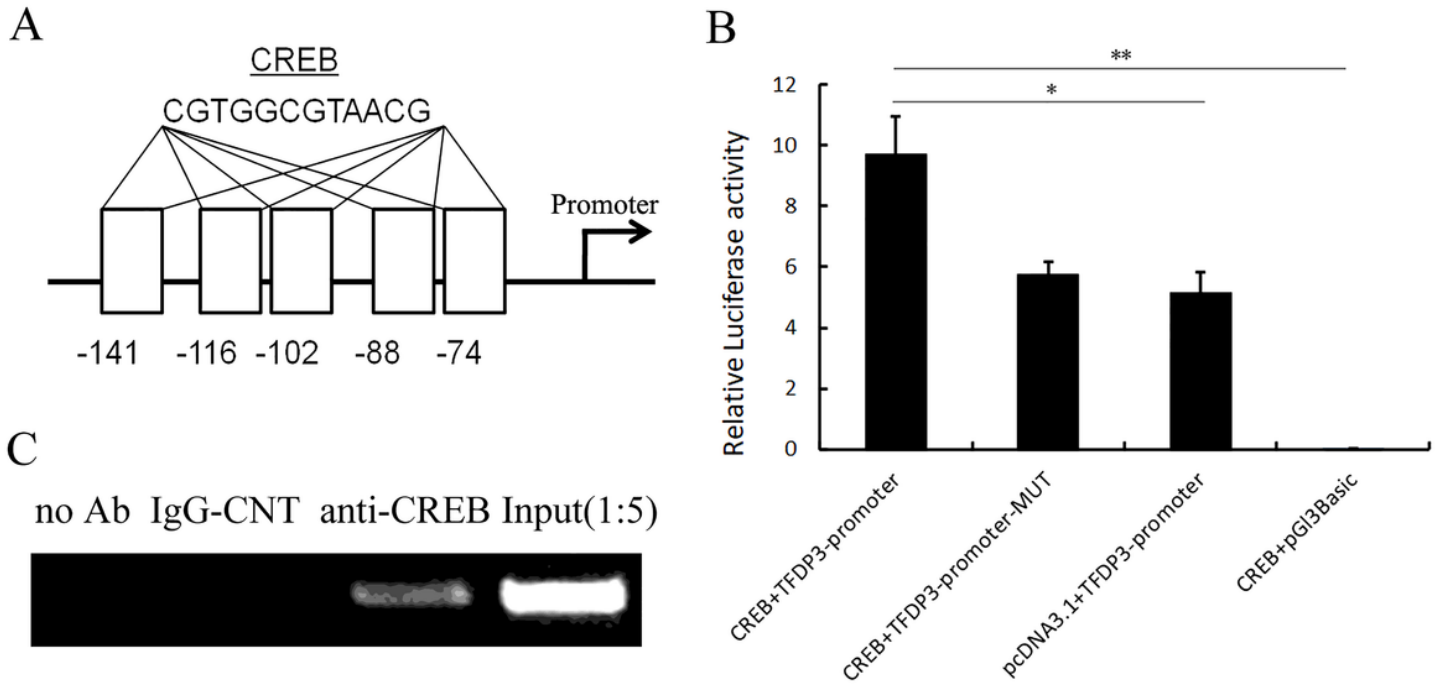

Figure 1

Luciferasereporterand ChIP assay analysis of the physical interaction between the putative CRE motif and the transcription factor, CREB. A. All constructs were transfected in the cells and the activity of the promoters was measured. The data are presented as the meanfirefly/Renilla luciferase ratio relative to the activity of the wild construct (designated as 100%). Eachpoint corresponds to the mean ± SD of three assays that were conducted in triplicate. The asterisks indicate statistical significance (P < 0.05) between the groups. B. ChIP assay was used to examine the interactionbetween the TFDP3 promoter and CREB. The experiments were conducted with chromatin derived from cell lines. Immunoprecipitated chromatin was used for the PCR assay usingspecific primers and the amplicon was resolved on a 3% agarose gel. The input DNA was used as a positive control for amplification. C. Schematic chart of the binding sites up-stream of the TFDP3 promoter.

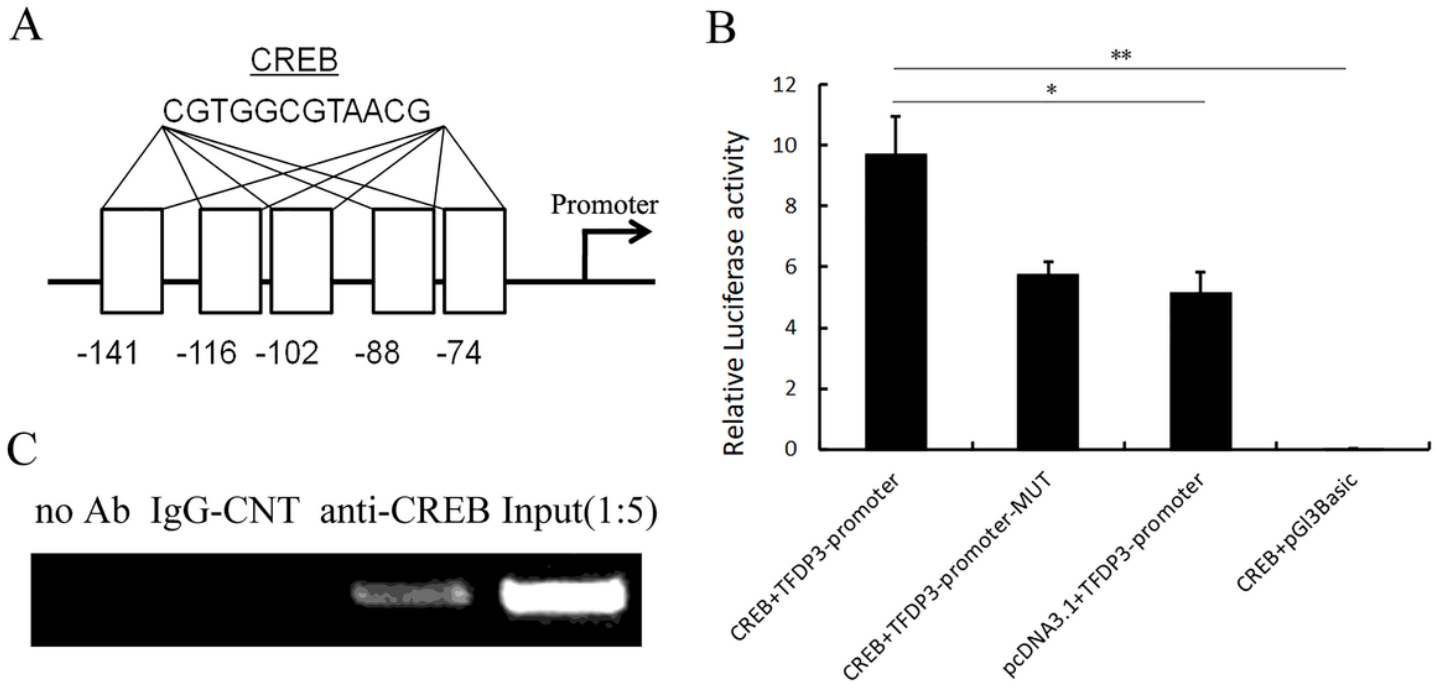

Figure 1

Luciferasereporterand ChIP assay analysis of the physical interaction between the putative CRE motif and the transcription factor, CREB. A. All constructs were transfected in the cells and the activity of the promoters was measured. The data are presented as the meanfirefly/Renilla luciferase ratio relative to the activity of the wild construct (designated as 100%). Eachpoint corresponds to the mean ± SD of three assays that were conducted in triplicate. The asterisks indicate statistical significance ($P < 0.05$) between the groups. B. ChIP assay was used to examine the interactionbetween the TFDP3 promoter and CREB. The experiments were conducted with chromatin derived from cell lines. Immunoprecipitated chromatin was used for the PCR assay usingspecific primers and the amplicon was resolved on a 3% agarose gel. The input DNA was used as a positive control for amplification. C. Schematic chart of the binding sites up-stream of the TFDP3 promoter.

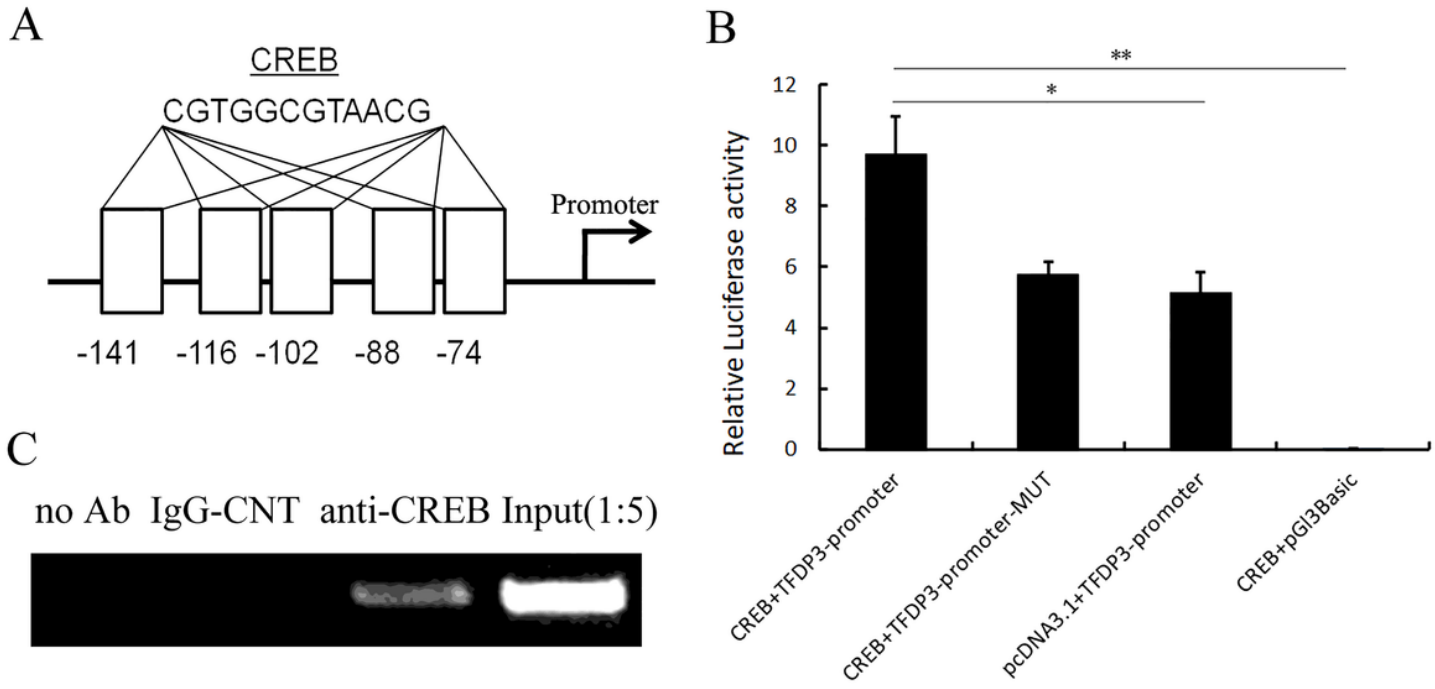

Figure 1

Luciferasereporterand ChIP assay analysis of the physical interaction between the putative CRE motif and the transcription factor, CREB. A. All constructs were transfected in the cells and the activity of the promoters was measured. The data are presented as the meanfirefly/Renilla luciferase ratio relative to the activity of the wild construct (designated as 100%). Eachpoint corresponds to the mean ± SD of three assays that were conducted in triplicate. The asterisks indicate statistical significance ($P < 0.05$) between the groups. B. ChIP assay was used to examine the interactionbetween the TFDP3 promoter and CREB. The experiments were conducted with chromatin derived from cell lines. Immunoprecipitated chromatin was used for the PCR assay usingspecific primers and the amplicon was resolved on a 3% agarose gel. The input DNA was used as a positive control for amplification. C. Schematic chart of the binding sites up-stream of the TFDP3 promoter.

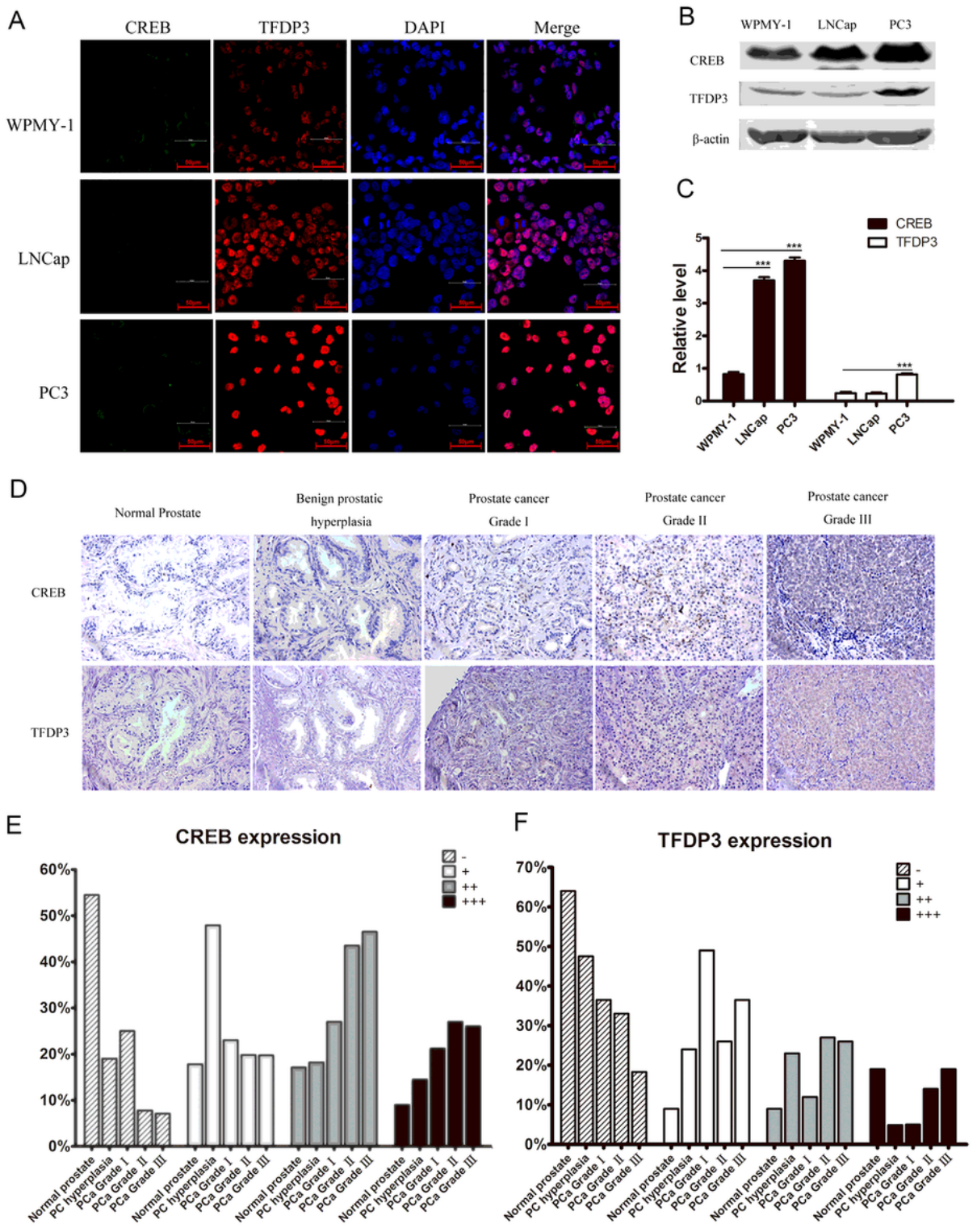

Figure 2

Expression of TFDP3 and CREB in prostate cells and tissue. A: ICF of CREB and TFDP3 in WPMY-1, PC3 and LNCap cells; B: Western blotting for CREB and TFDP3 in WPMY-1, PC3 and LNCap cells. C: Quantification of CREB and TFDP3 western blotting analysis in WPMY-1,PC3 and LNCap cells, n=3. D: TFDP3 and CREB were detected (browncolor) using anti-TFDP3 and anti-CREB antibodies in tissues of normal prostate, prostatichyperplasia and prostate cancer by IHC. E. Quantification of CREB expression

levels in samples of different pathologicalgrades and clinical stages. F. Quantification ofTFDP3 expression in samples of different pathologicalgrades and clinical stages.

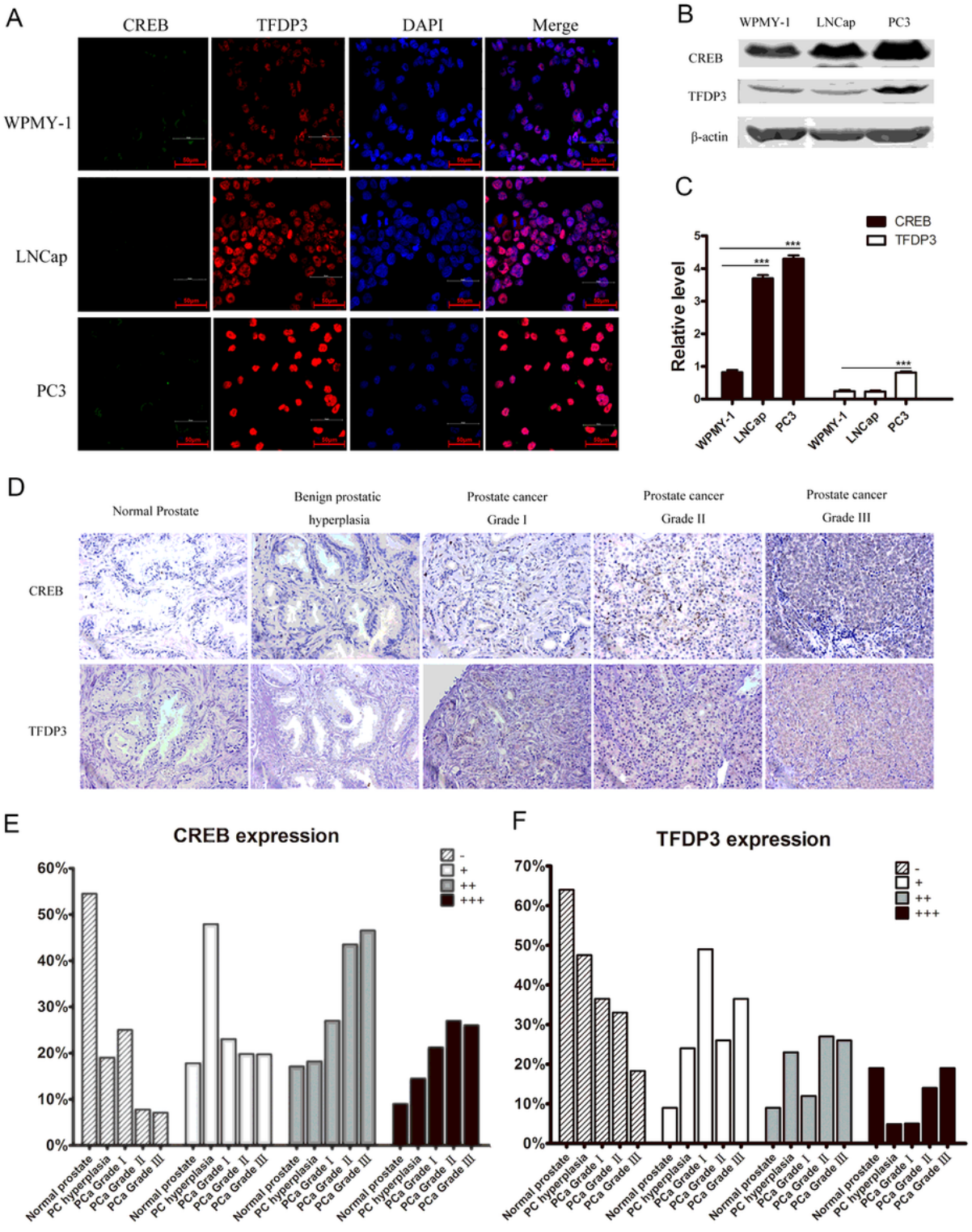

Figure 2

Expression of TFDP3 and CREB in prostate cells and tissue. A: ICF of CREB and TFDP3 in WPMY-1, PC3 and LNCap cells; B: Western blotting for CREB and TFDP3 in WPMY-1, PC3 and LNCap cells. C: Quantification of CREB and TFDP3 western blotting analysis in WPMY-1,PC3 and LNCap cells, n=3. D:

TFDP3 and CREB were detected (browncolor) using anti-TFDP3 and anti-CREB antibodies in tissues of normal prostate, prostatichyperplasia and prostate cancer by IHC. E. Quantification of CREB expression levels in samples of different pathologicalgrades and clinical stages. F. Quantification ofTFDP3 expression in samples of different pathologicalgrades and clinical stages.

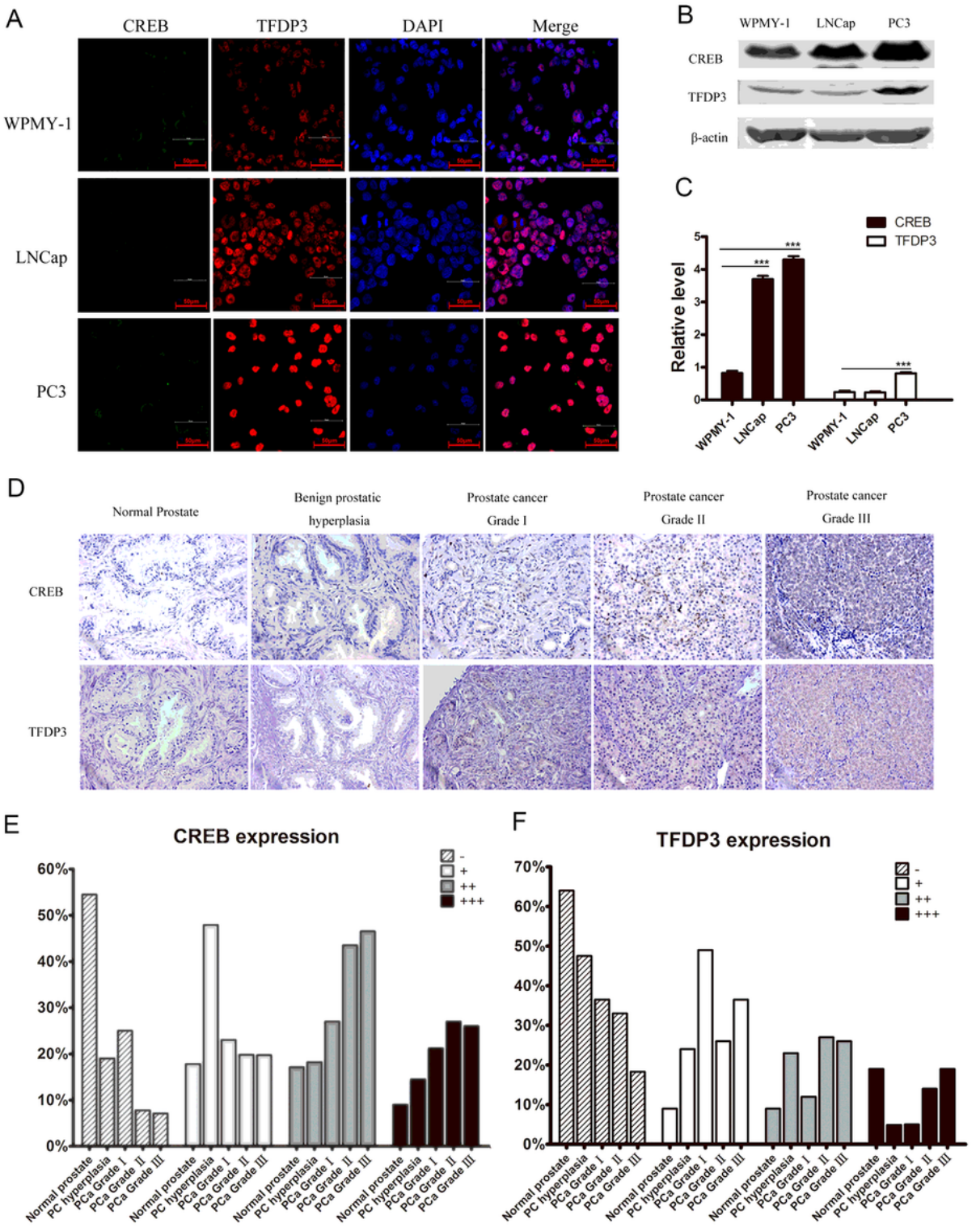

Figure 2

Expression of TFDP3 and CREB in prostate cells and tissue. A: ICF of CREB and TFDP3 in WPMY-1, PC3 and LNCap cells; B: Western blotting for CREB and TFDP3 in WPMY-1, PC3 and LNCap cells. C: Quantification of CREB and TFDP3 western blotting analysis in WPMY-1,PC3 and LNCap cells, n=3. D: TFDP3 and CREB were detected (browncolor) using anti-TFDP3 and anti-CREB antibodies in tissues of normal prostate, prostatichyperplasia and prostate cancer by IHC. E. Quantification of CREB expression levels in samples of different pathologicalgrades and clinical stages. F. Quantification ofTFDP3 expression in samples of different pathologicalgrades and clinical stages.

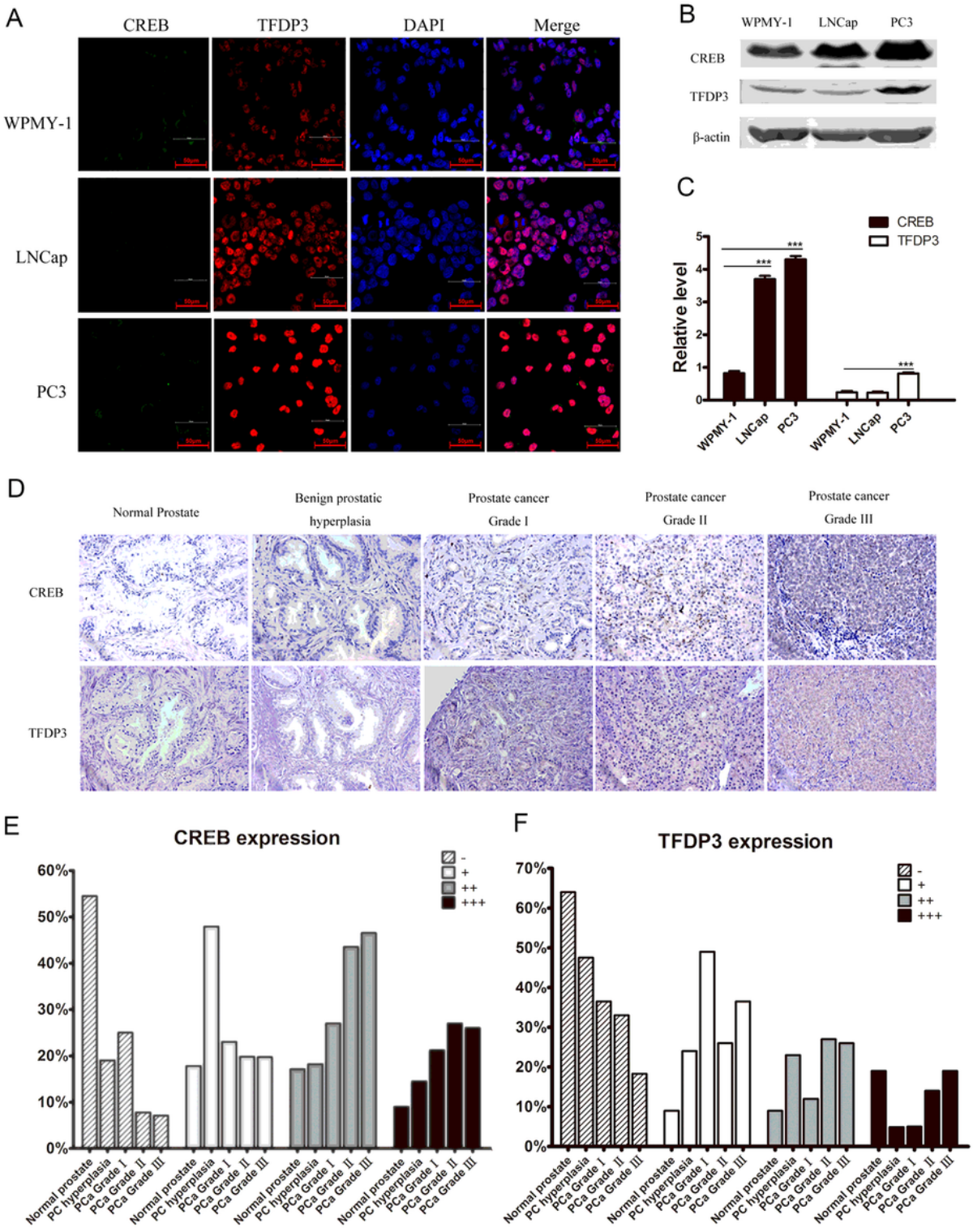

Figure 2

Expression of TFDP3 and CREB in prostate cells and tissue. A: ICF of CREB and TFDP3 in WPMY-1, PC3 and LNCap cells; B: Western blotting for CREB and TFDP3 in WPMY-1, PC3 and LNCap cells. C: Quantification of CREB and TFDP3 western blotting analysis in WPMY-1,PC3 and LNCap cells, n=3. D: TFDP3 and CREB were detected (browncolor) using anti-TFDP3 and anti-CREB antibodies in tissues of normal prostate, prostatichyperplasia and prostate cancer by IHC. E. Quantification of CREB expression levels in samples of different pathologicalgrades and clinical stages. F. Quantification ofTFDP3 expression in samples of different pathologicalgrades and clinical stages.

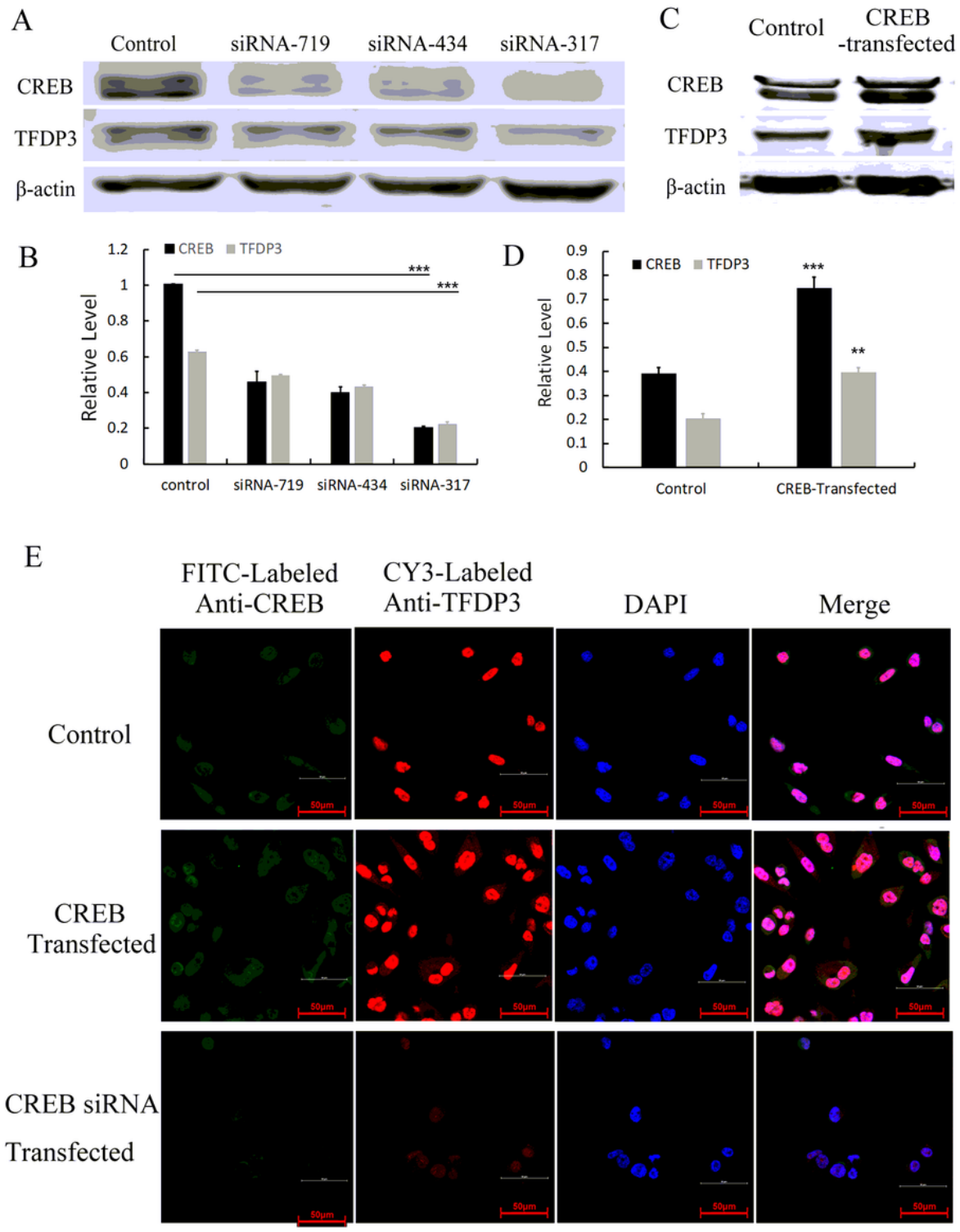

Figure 3

The effects of CREB treatment and site-directed mutagenesis on the expression and activity of the TFDP3 promoter. A. Analysis of the expression of TFDP3 after CREB silencingC. Following CREB transfection, the levels of the TFDP3 protein were determined by Western blotting. B and D the expression of CREB and TFDP3 were respectively quantifiedfor A and C.Compared with control, TFDP3 was significantly increased

after CREB transfection.**P<0.01. E. ICFfor CREB and TFDP3 in PC3 cells,following CREB plasmid and/or CREB-siRNAtransfection. FITC and CY3 wereusedin order to label TFDP3 and CREB, respectively.

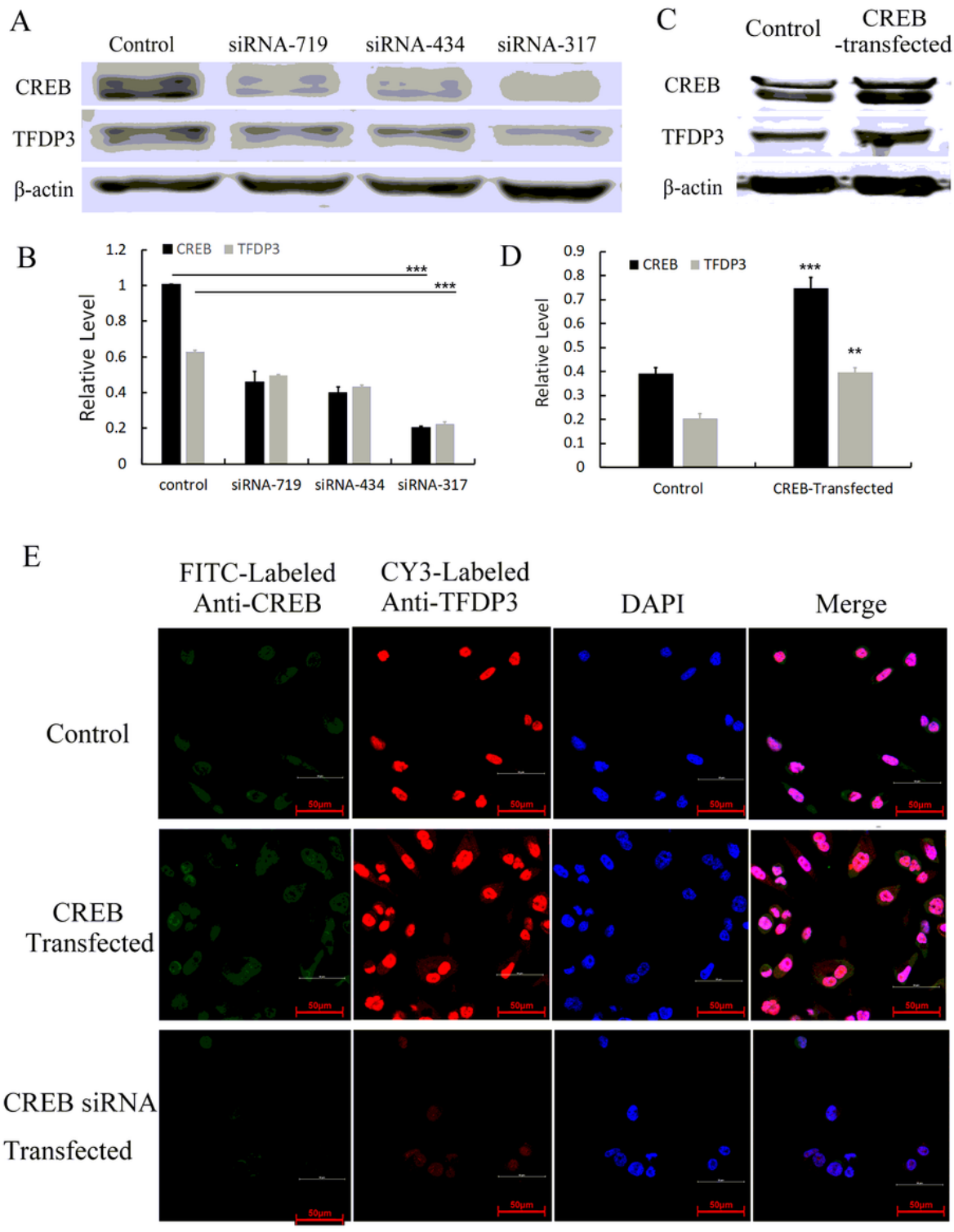

Figure 3

The effects of CREB treatment and site-directed mutagenesis on the expression and activity of the TFDP3 promoter. A. Analysis of the expression of TFDP3 after CREB silencingC. Following CREB transfection, the levels of the TFDP3 protein were determined by Western blotting. B and D the expression of CREB and

TFDP3 were respectively quantifiedfor A and C.Compared with control, TFDP3 was significantly increased after CREB transfection.**P<0.01. E. ICFfor CREB and TFDP3 in PC3 cells,following CREB plasmid and/or CREB-siRNAtransfection. FITC and CY3 wereusedin order to label TFDP3 and CREB, respectively.

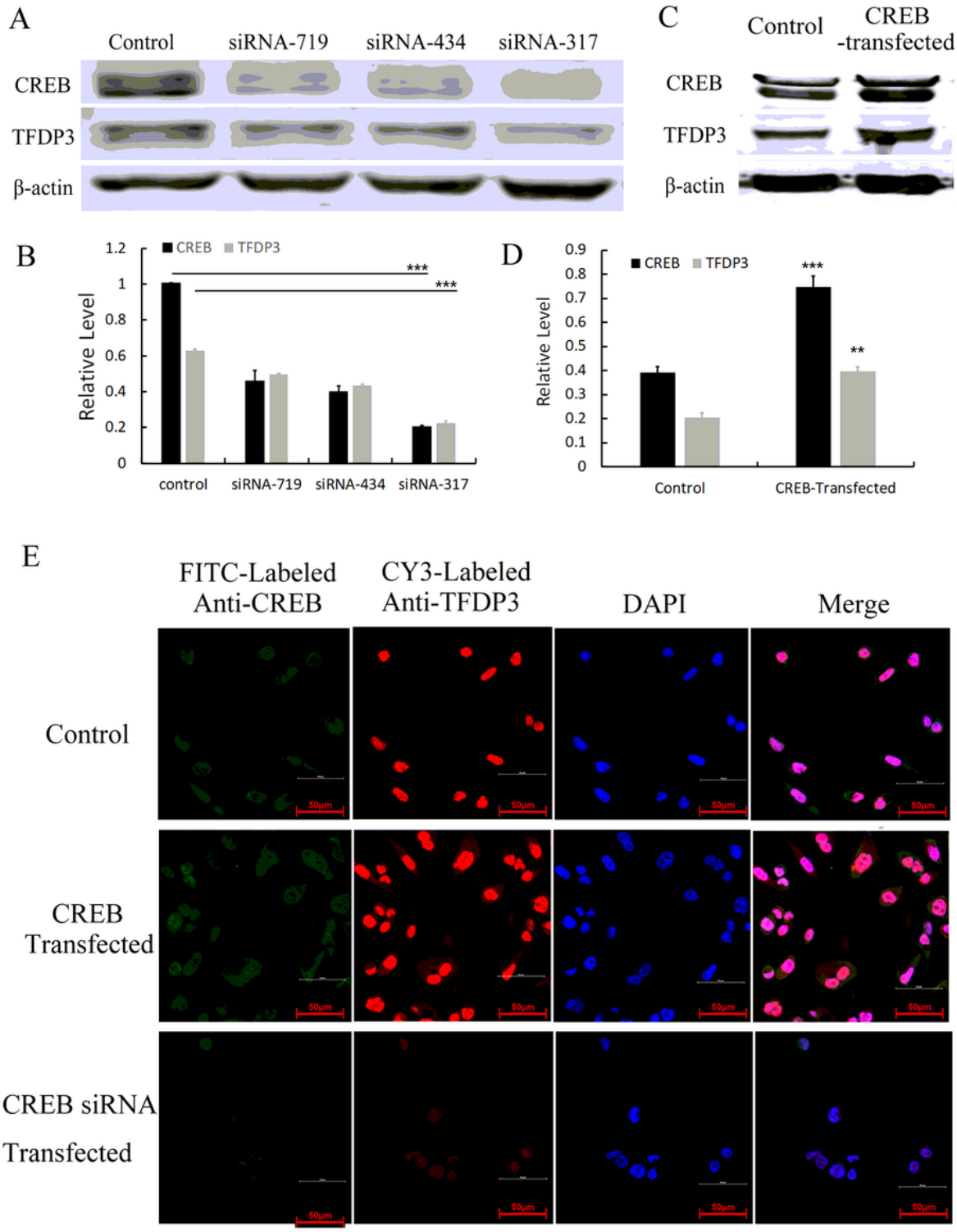

Figure 3

The effects of CREB treatment and site-directed mutagenesis on the expression and activity of the TFDP3 promoter. A. Analysis of the expression of TFDP3 after CREB silencingC. Following CREB transfection, the

levels of the TFDP3 protein were determined by Western blotting. B and D the expression of CREB and TFDP3 were respectively quantifiedfor A and C.Compared with control, TFDP3 was significantly increased after CREB transfection.**P<0.01. E. ICFfor CREB and TFDP3 in PC3 cells,following CREB plasmid and/or CREB-siRNAtransfection. FITC and CY3 wereusedin order to label TFDP3 and CREB, respectively.

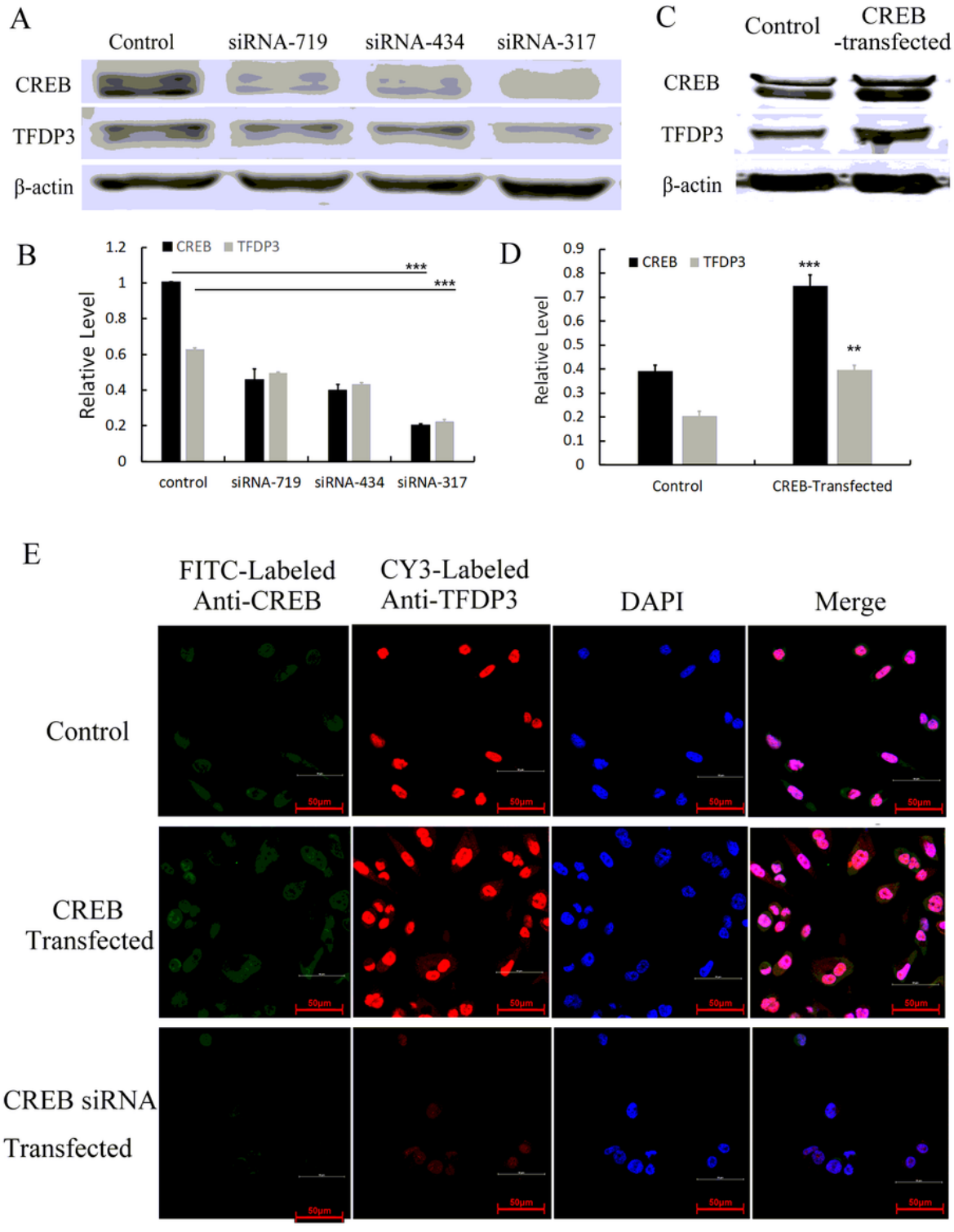

Figure 3

The effects of CREB treatment and site-directed mutagenesis on the expression and activity of the TFDP3 promoter. A. Analysis of the expression of TFDP3 after CREB silencingC. Following CREB transfection, the levels of the TFDP3 protein were determined by Western blotting. B and D the expression of CREB and TFDP3 were respectively quantifiedfor A and C.Compared with control, TFDP3 was significantly increased after CREB transfection.**P<0.01. E. ICFfor CREB and TFDP3 in PC3 cells,following CREB plasmid and/or CREB-siRNAtransfection. FITC and CY3 wereusedin order to label TFDP3 and CREB, respectively.

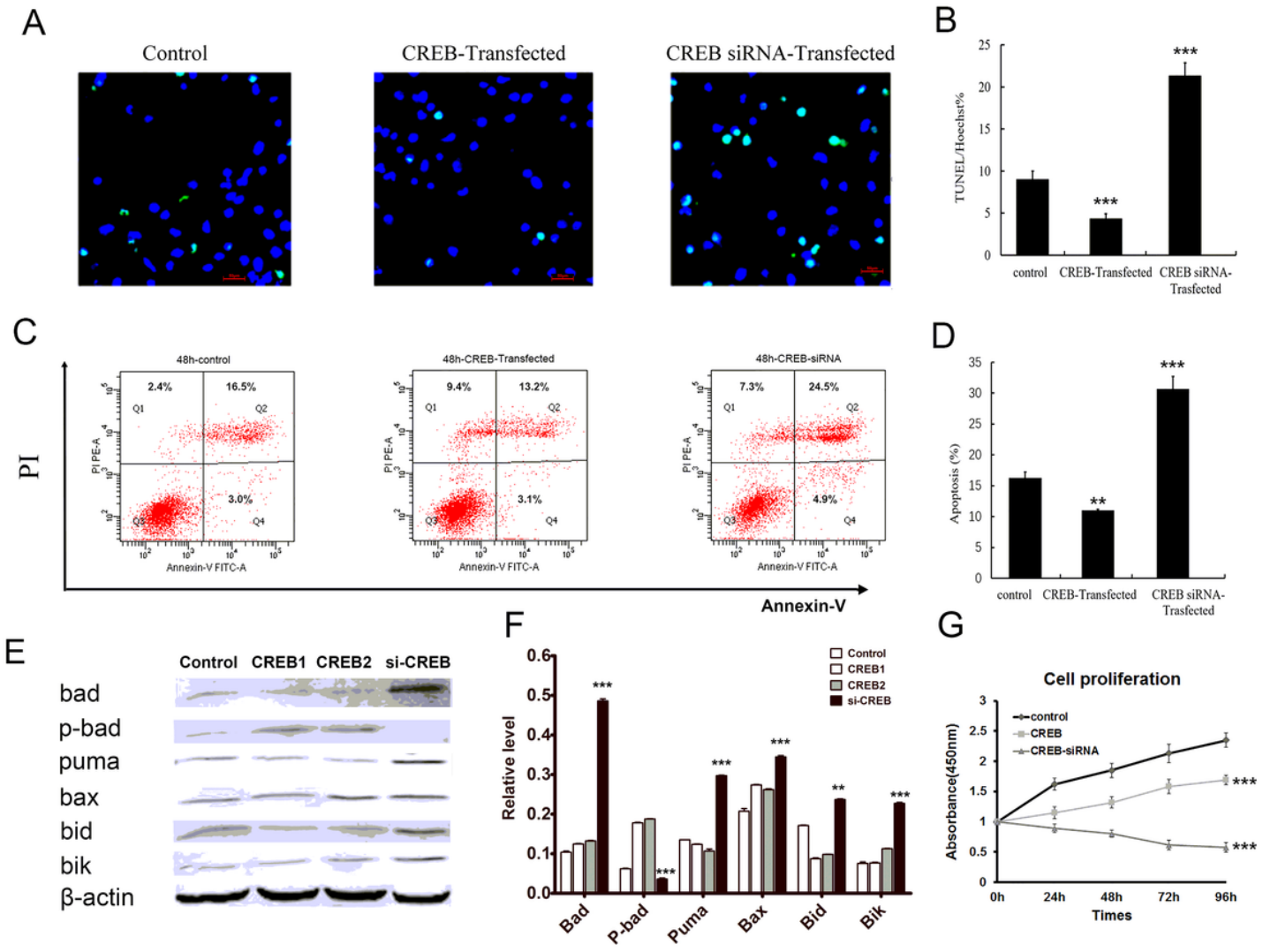

Figure 4

Effect of CREB on apoptosis and proliferation of prostate cancer cells. A and C. Apoptosis analysis of PC3 cells transfected with pcDNA3.1-CREB plasmid and CREB-siRNA were analyzed by TUNEL staining and the rate of total apoptosis were quantified..***P<0.001, n=3. B and D. Apoptosis analysis of PC3 cells transfected with pcDNA3.1-CREB plasmid and CREB-siRNA were analyzed by flow cytometry and the rate of total apoptosis were quantified.Statistical significance is indicated by asterisks and significant levels as**P<0.01, ***P<0.001, n=3 C. The CCK-8 assay was used for the detection of the effect of CREB on growth of PC3 cells by transfection of CREB-siRNA and pcDNA3.1-CREB plasmid,***P<0.001, n=3.

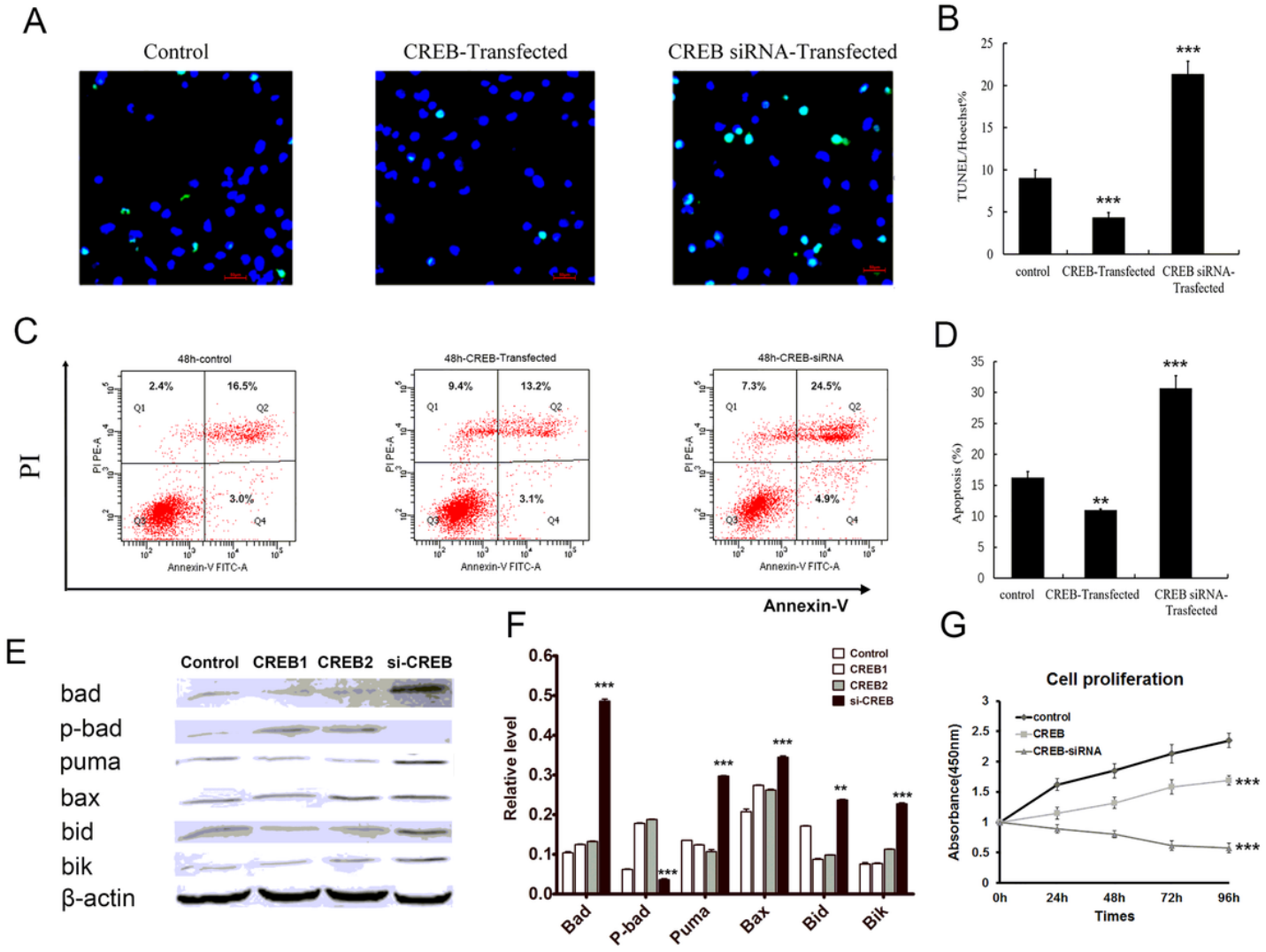

Figure 4

Effect of CREB on apoptosis and proliferation of prostate cancer cells. A and C. Apoptosis analysis of PC3 cells transfected with pcDNA3.1-CREB plasmid and CREB-siRNA were analyzed by TUNEL staining and the rate of total apoptosis were quantified..***P<0.001, n=3. B and D. Apoptosis analysis of PC3 cells transfected with pcDNA3.1-CREB plasmid and CREB-siRNA were analyzed by flow cytometry and the rate of total apoptosis were quantified.Statistical significance is indicated by asterisks and significant levels as**P<0.01, ***P<0.001, n=3 C. The CCK-8 assay was used for the detection of the effect of CREB on growth of PC3 cells by transfection of CREB-siRNA and pcDNA3.1-CREB plasmid,***P<0.001, n=3.

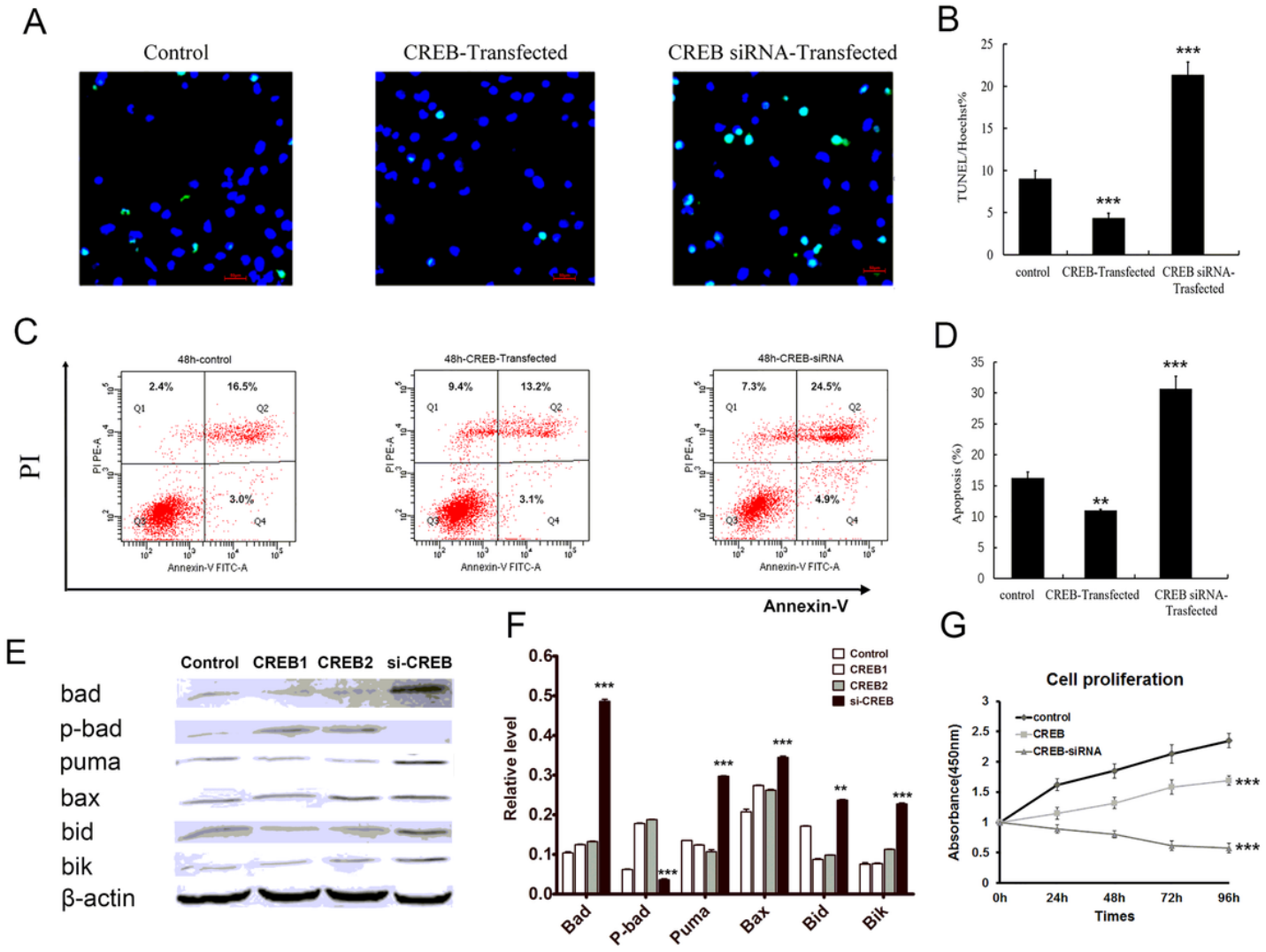

Figure 4

Effect of CREB on apoptosis and proliferation of prostate cancer cells. A and C. Apoptosis analysis of PC3 cells transfected with pcDNA3.1-CREB plasmid and CREB-siRNA were analyzed by TUNEL staining and the rate of total apoptosis were quantified..***P<0.001, n=3. B and D. Apoptosis analysis of PC3 cells transfected with pcDNA3.1-CREB plasmid and CREB-siRNA were analyzed by flow cytometry and the rate of total apoptosis were quantified.Statistical significance is indicated by asterisks and significant levels as**P<0.01, ***P<0.001, n=3 C. The CCK-8 assay was used for the detection of the effect of CREB on growth of PC3 cells by transfection of CREB-siRNA and pcDNA3.1-CREB plasmid,***P<0.001, n=3.

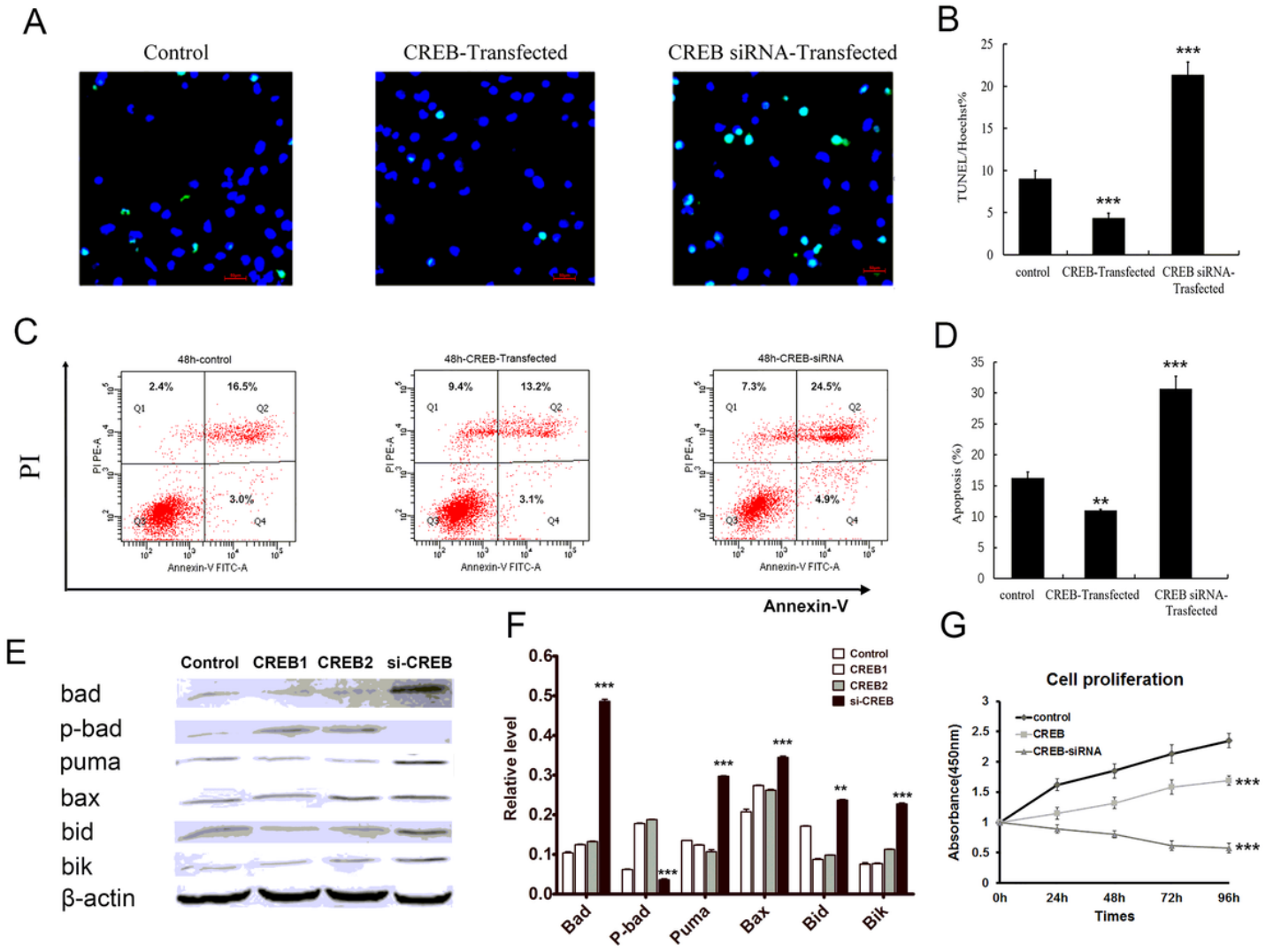

Figure 4

Effect of CREB on apoptosis and proliferation of prostate cancer cells. A and C. Apoptosis analysis of PC3 cells transfected with pcDNA3.1-CREB plasmid and CREB-siRNA were analyzed by TUNEL staining and the rate of total apoptosis were quantified..***P<0.001, n=3. B and D. Apoptosis analysis of PC3 cells transfected with pcDNA3.1-CREB plasmid and CREB-siRNA were analyzed by flow cytometry and the rate of total apoptosis were quantified.Statistical significance is indicated by asterisks and significant levels as**P<0.01, ***P<0.001, n=3 C. The CCK-8 assay was used for the detection of the effect of CREB on growth of PC3 cells by transfection of CREB-siRNA and pcDNA3.1-CREB plasmid,***P<0.001, n=3.

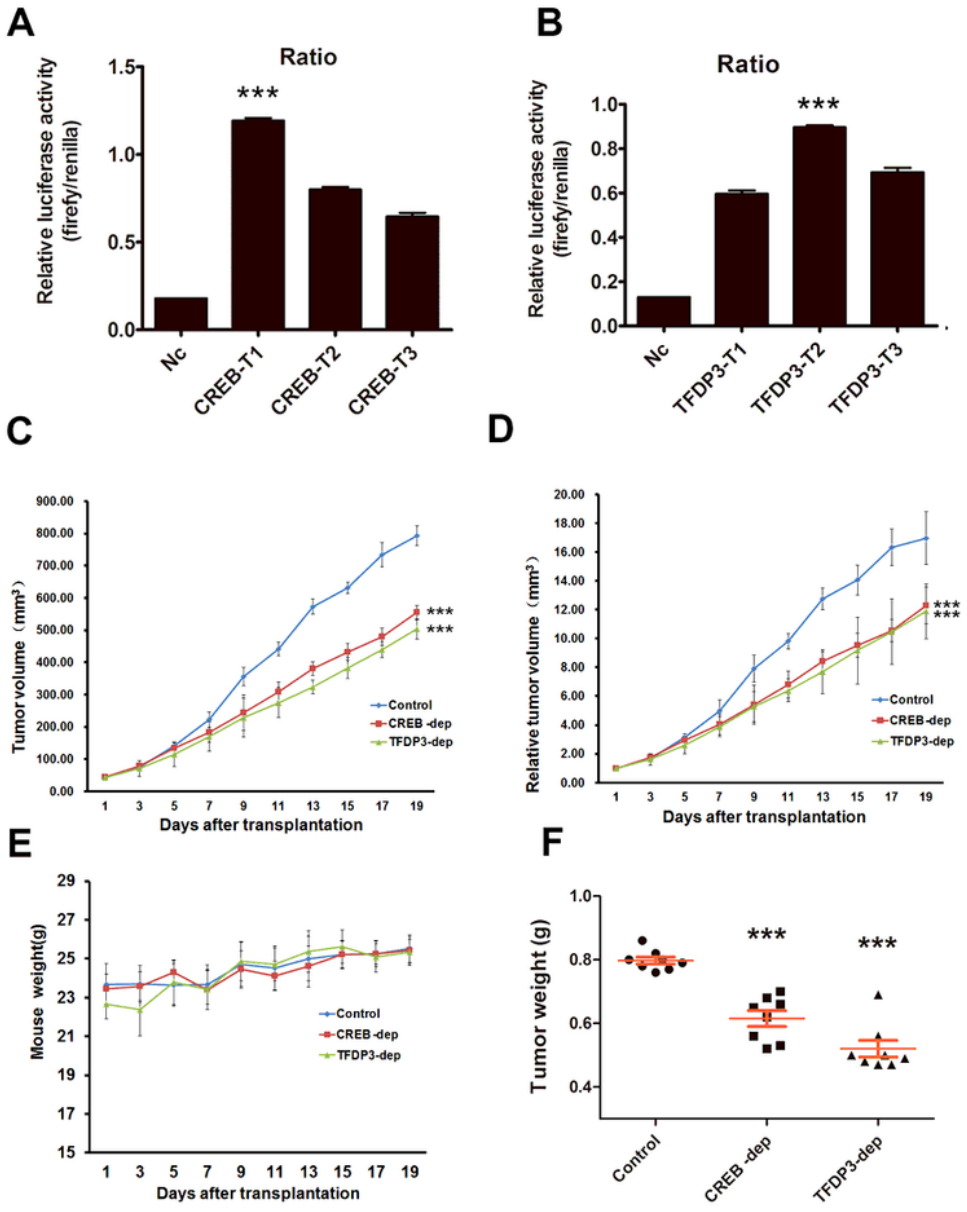

Figure 5

The knockout of CREB and TDFP3 inhibited the growth of PC3 in xenograftsofathymic mice.A and B: CREB-dep and TDFP3-dep were performed by CRISPR / cas9 and the activity was detected by Luciferase SSA. The strongest fluorescence vectors were selected, as LentiCRISPR-CREB1-T1 and lentiCRISPR-TFDP3-T2. C and D. The volumes and relative tumor volumes (RTV) of PC3, PC3 with lentiCRISPR-CREB(CREB-dep) and PC3 with lentiCRISPR-TFDP3(TFDP3-dep) xenografts were measured or calculated

every 2 days. Compared with the control group, the difference of tumor volume and RTV became significant after day 7 in CREB-dep and TFDP3-dep group (***P<0.001, Student'st-testtreatment vs. control). E. Changes in body weight of mice are shown in different groups. F. Tumor weight distribution in each group at the end of the experiment. Red lines indicatedaverage tumor weight.Statistical significance is indicated by asterisks and significant levels as ***P<0.001.

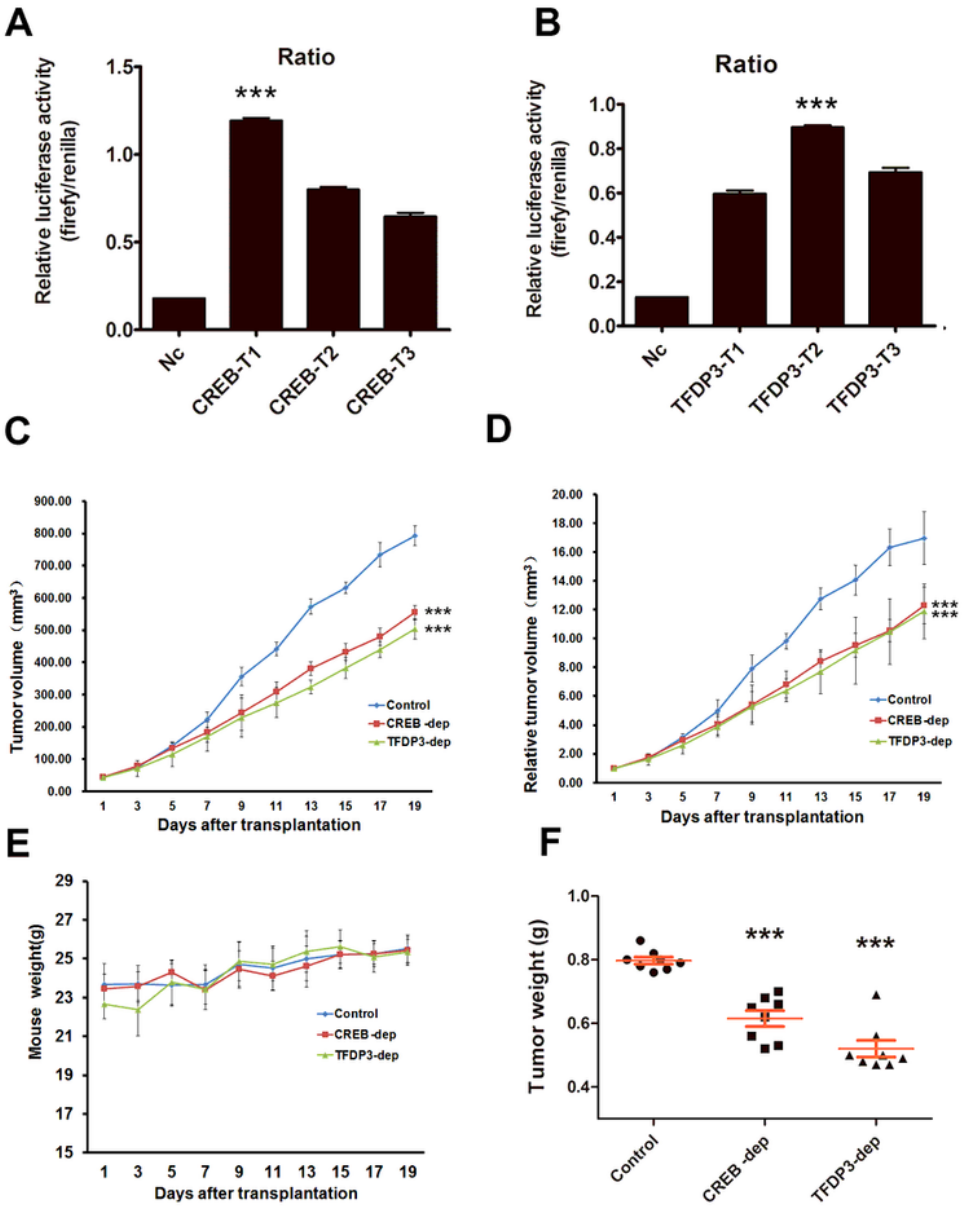

Figure 5

The knockout of CREB and TDFP3 inhibited the growth of PC3 in xenograftsofathymic mice.A and B: CREB-dep and TDFP3-dep were performed by CRISPR / cas9 and the activity was detected by Luciferase SSA. The strongest fluorescence vectors were selected, as LentiCRISPR-CREB1-T1 and lentiCRISPR-TFDP3-T2. C and D. The volumes and relative tumor volumes (RTV) of PC3, PC3 with lentiCRISPR-CREB(CREB-dep) and PC3 with lentiCRISPR-TFDP3(TFDP3-dep) xenografts were measured or calculated every 2 days. Compared with the control group, the difference of tumor volume and RTV became significant after day 7 in CREB-dep and TFDP3-dep group (***P<0.001, Student'st-testtreatment vs. control). E. Changes in body weight of mice are shown in different groups. F. Tumor weight distribution in each group at the end of the experiment. Red lines indicatedaverage tumor weight.Statistical significance is indicated by asterisks and significant levels as ***P<0.001.

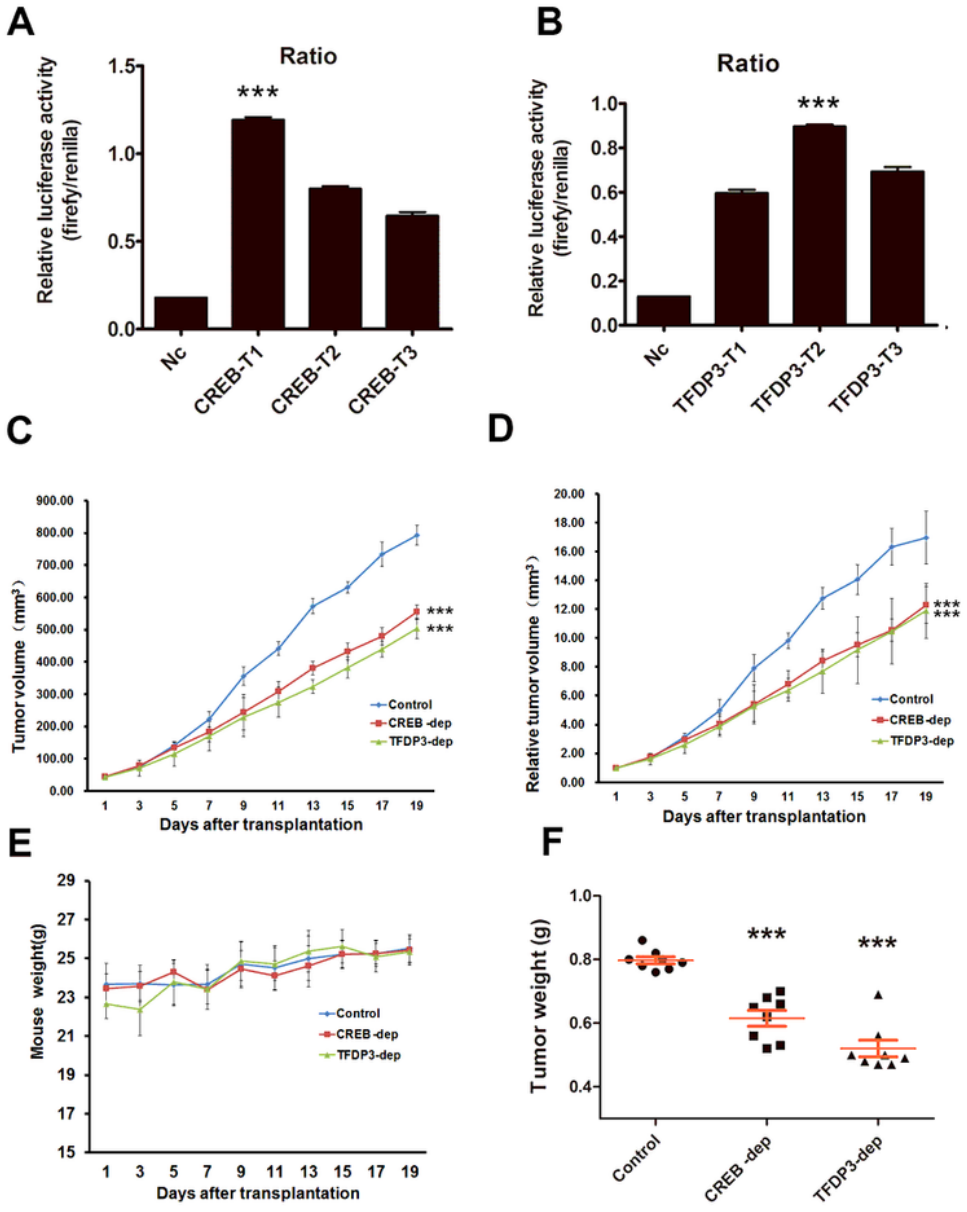

Figure 5

The knockout of CREB and TDFP3 inhibited the growth of PC3 in xenograftsofathymic mice.A and B: CREB-dep and TDFP3-dep were performed by CRISPR / cas9 and the activity was detected by Luciferase SSA. The strongest fluorescence vectors were selected, as LentiCRISPR-CREB1-T1 and lentiCRISPR-TFDP3-T2. C and D. The volumes and relative tumor volumes (RTV) of PC3, PC3 with lentiCRISPR-CREB(CREB-dep) and PC3 with lentiCRISPR-TFDP3(TFDP3-dep) xenografts were measured or calculated

every 2 days. Compared with the control group, the difference of tumor volume and RTV became significant after day 7 in CREB-dep and TFDP3-dep group (***P<0.001, Student'st-testtreatment vs. control). E. Changes in body weight of mice are shown in different groups. F. Tumor weight distribution in each group at the end of the experiment. Red lines indicatedaverage tumor weight.Statistical significance is indicated by asterisks and significant levels as ***P<0.001.

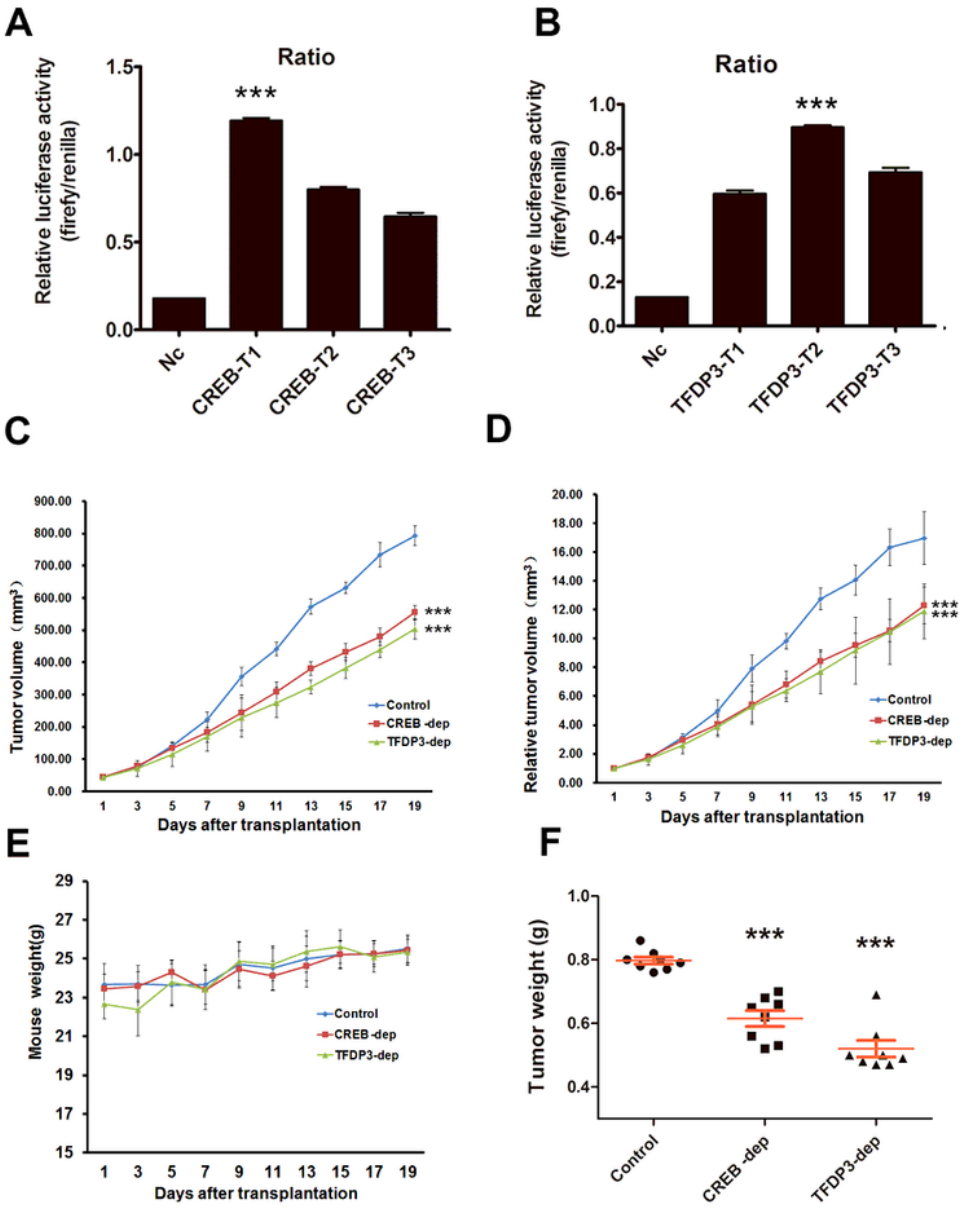

Figure 5

The knockout of CREB and TDFP3 inhibited the growth of PC3 in xenograftsofathymic mice.A and B: CREB-dep and TDFP3-dep were performed by CRISPR / cas9 and the activity was detected by Luciferase SSA. The strongest fluorescence vectors were selected, as LentiCRISPR-CREB1-T1 and lentiCRISPR-TFDP3-T2. C and D. The volumes and relative tumor volumes (RTV) of PC3, PC3 with lentiCRISPR-CREB(CREB-dep) and PC3 with lentiCRISPR-TFDP3(TFDP3-dep) xenografts were measured or calculated every 2 days. Compared with the control group, the difference of tumor volume and RTV became significant after day 7 in CREB-dep and TFDP3-dep group (***P<0.001, Student'st-testtreatment vs. control). E. Changes in body weight of mice are shown in different groups. F. Tumor weight distribution in each group at the end of the experiment. Red lines indicatedaverage tumor weight.Statistical significance is indicated by asterisks and significant levels as ***P<0.001.

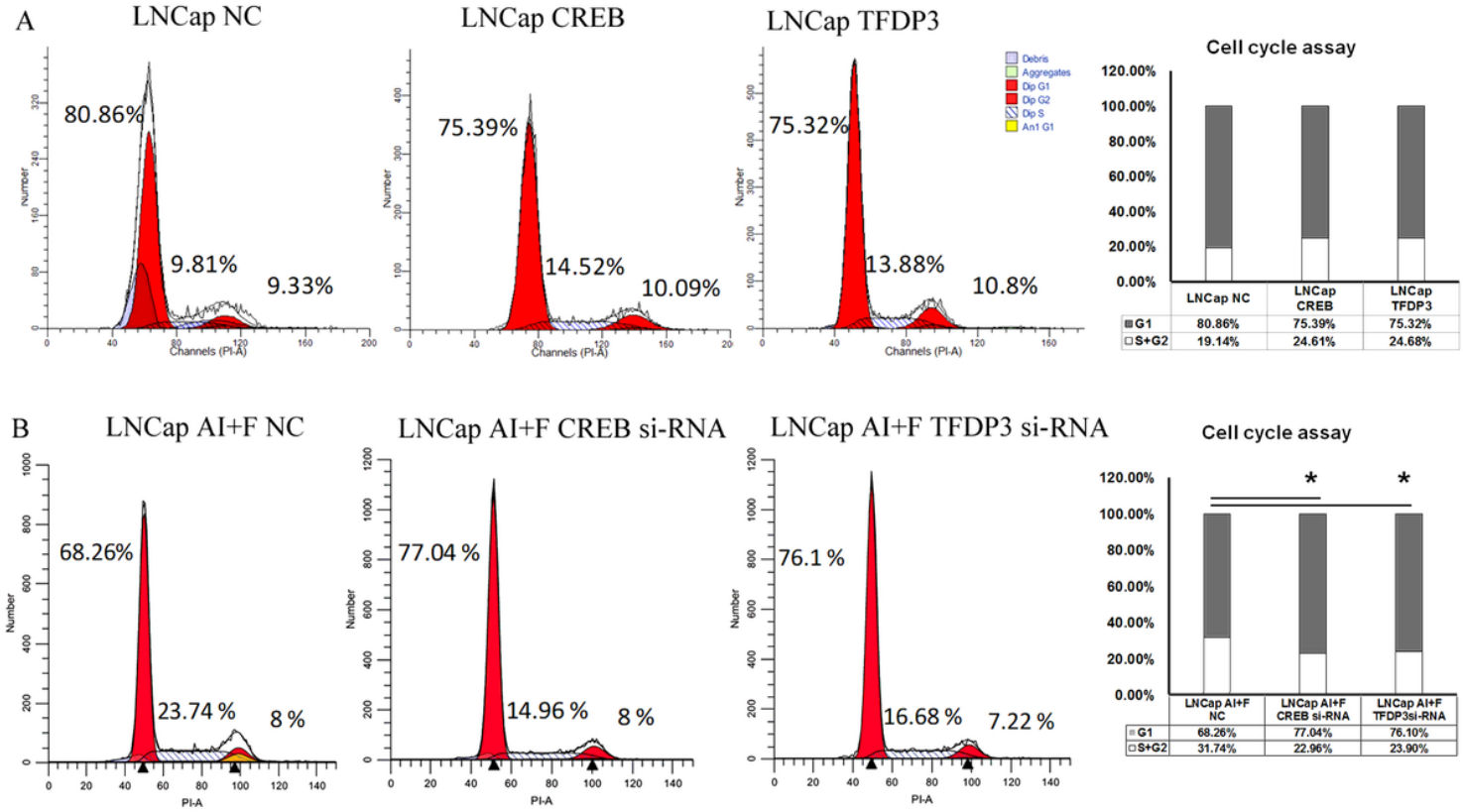

Figure 6

The overexpression and silence of CREB and TFDP3 could lead to the G1/S transition in LNCaPandLNCaP AI+F cellA. Overexpression of CREB and TFDP3 accelerates the G1 phase of the cell cycle. B. The silenceof CREB and TFDP3 could lead to substantial accumulation of the cell population at the G1 stage of the cell cycle in LNCaP AI+F cells(P=0.015 and 0.010, respectively).

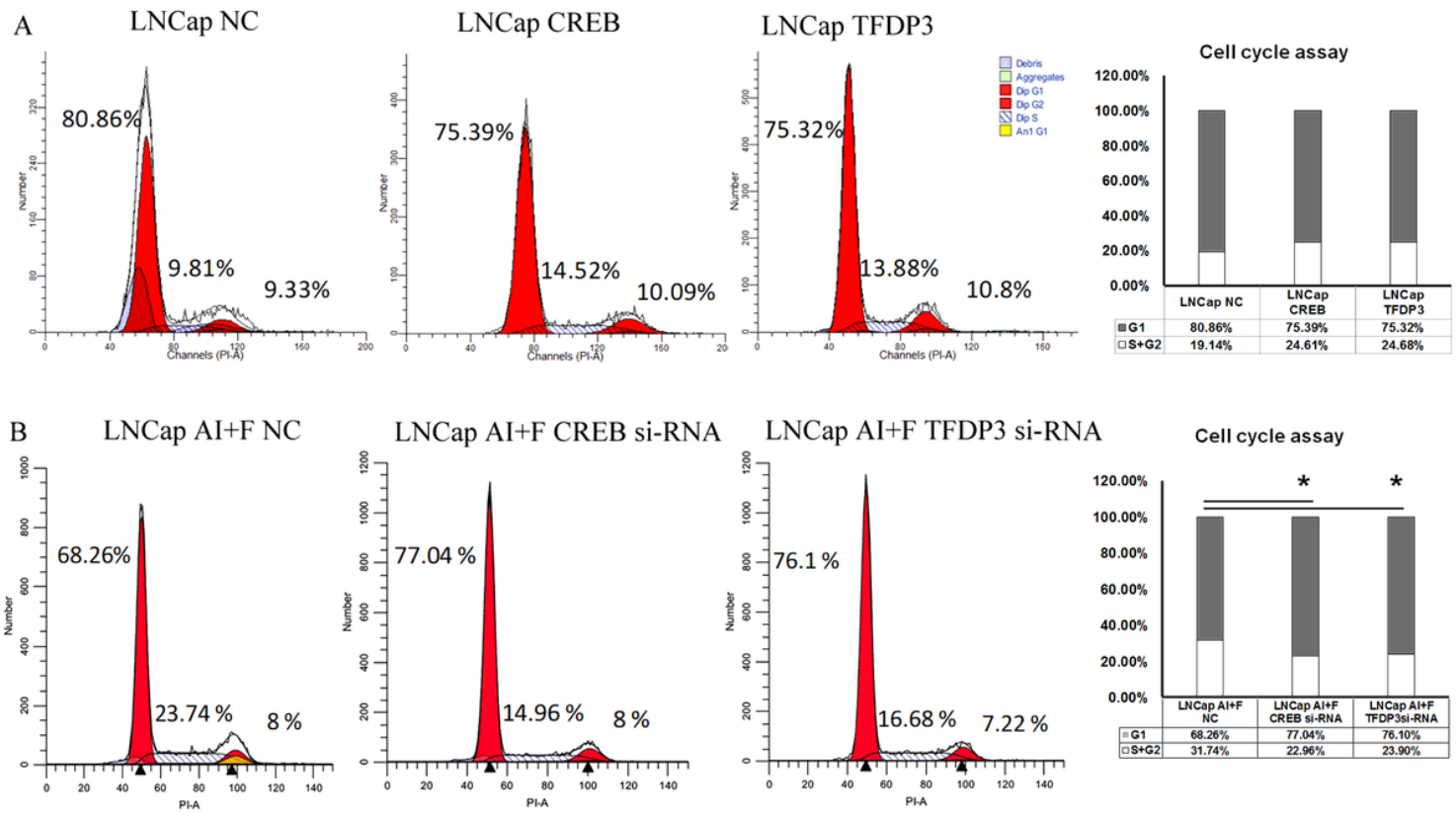

Figure 6

The overexpression and silence of CREB and TFDP3 could lead to the G1/S transition in LNCaPandLNCaP AI+F cellA. Overexpression of CREB and TFDP3 accelerates the G1 phase of the cell cycle. B. The silenceof CREB and TFDP3 could lead to substantial accumulation of the cell population at the G1 stage of the cell cycle in LNCaP AI+F cells(P=0.015 and 0.010, respectively).

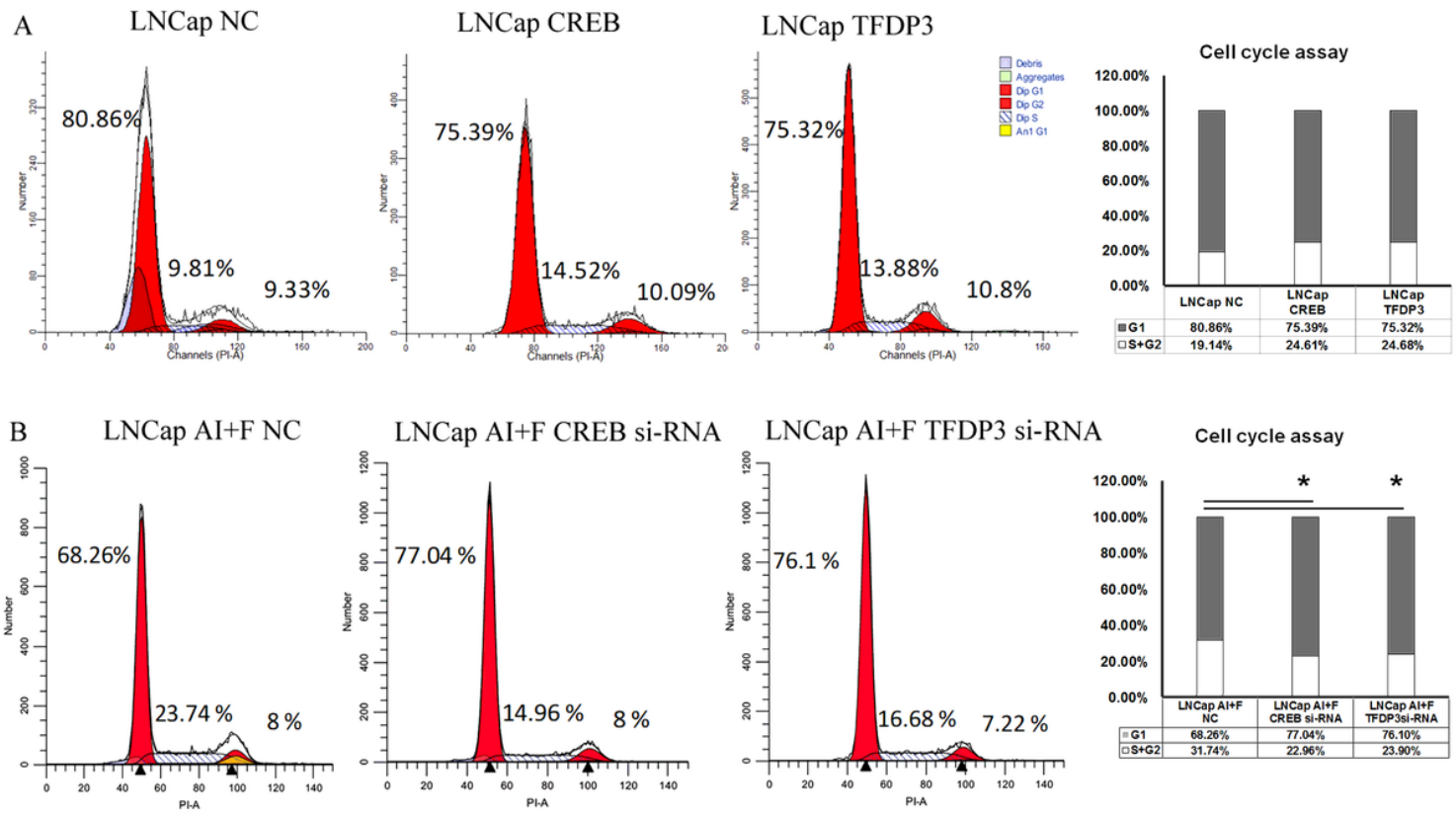

Figure 6

The overexpression and silence of CREB and TFDP3 could lead to the G1/S transition in LNCaPandLNCaP AI+F cellA. Overexpression of CREB and TFDP3 accelerates the G1 phase of the cell cycle. B. The silenceof CREB and TFDP3 could lead to substantial accumulation of the cell population at the G1 stage of the cell cycle in LNCaP AI+F cells(P=0.015 and 0.010, respectively).

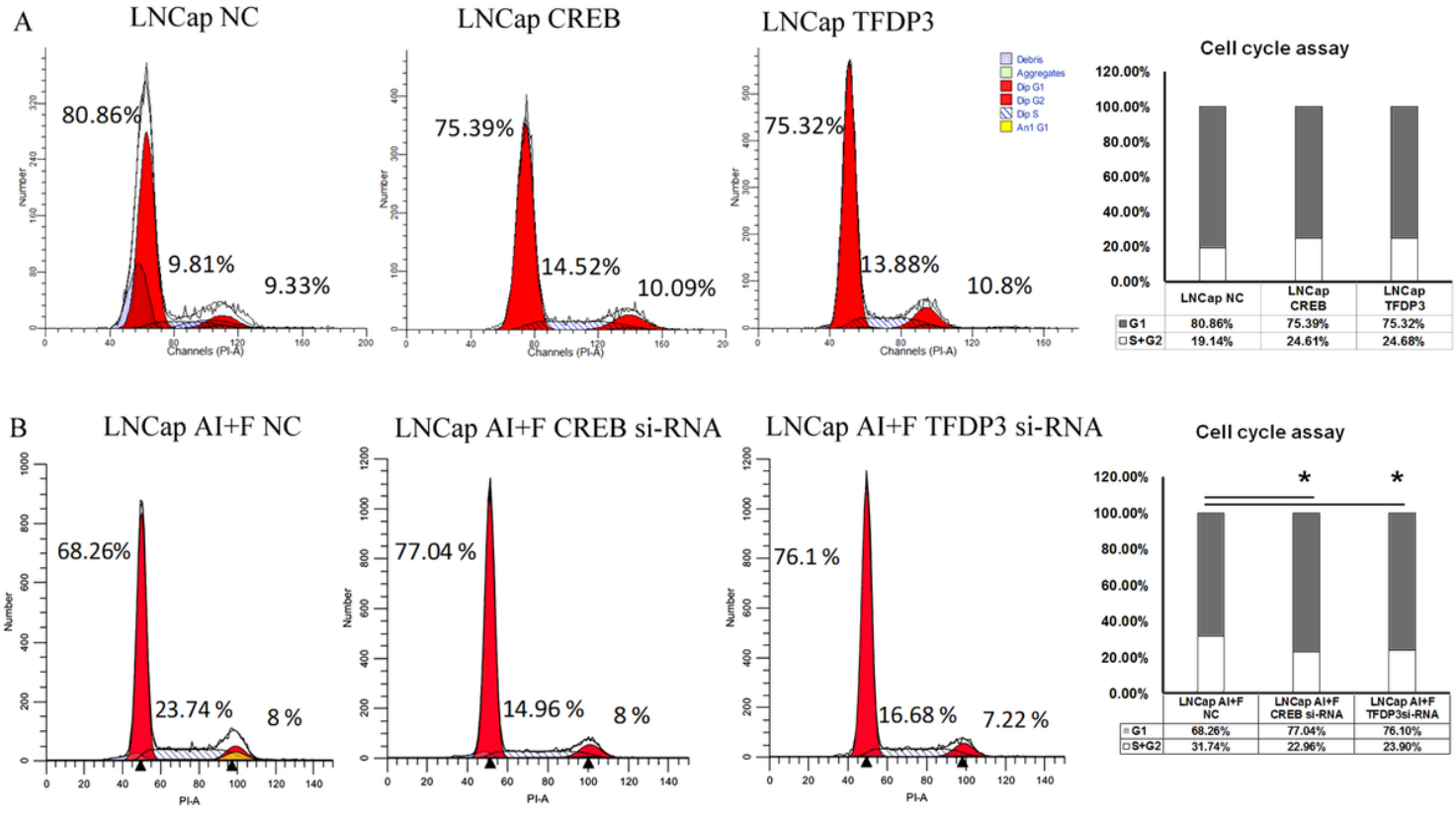

Figure 6

The overexpression and silence of CREB and TFDP3 could lead to the G1/S transition in LNCaPandLNCaP AI+F cellA. Overexpression of CREB and TFDP3 accelerates the G1 phase of the cell cycle. B. The silenceof CREB and TFDP3 could lead to substantial accumulation of the cell population at the G1 stage of the cell cycle in LNCaP AI+F cells(P=0.015 and 0.010, respectively).

Supplementary Files

This is a list of supplementary files associated with this preprint. Click to download.

- Supplementarydata.docx
- Supplementarydata.docx
- Supplementarydata.docx
- Supplementarydata.docx